

Electroweak Precision Observables, New Physics and the Nature of a 126 GeV Higgs Boson

Marco Ciuchini,^a Enrico Franco,^b Satoshi Mishima^{b,c} and Luca Silvestrini^b

^a*INFN, Sezione di Roma Tre, Via della Vasca Navale 84, I-00146 Roma, Italy*

^b*INFN, Sezione di Roma, Piazzale A. Moro 2, I-00185 Roma, Italy*

^c*Dipartimento di Fisica, Università di Roma “La Sapienza”,
Piazzale A. Moro 2, I-00185 Roma, Italy*

ABSTRACT: We perform the fit of electroweak precision observables within the Standard Model with a 126 GeV Higgs boson, compare the results with the theoretical predictions and discuss the impact of recent experimental and theoretical improvements. We introduce New Physics contributions in a model-independent way and fit for the S , T and U parameters, for the $\epsilon_{1,2,3,b}$ ones, for modified $Zb\bar{b}$ couplings and for a modified Higgs coupling to vector bosons. We point out that composite Higgs models are very strongly constrained. Finally, we compute the bounds on dimension-six operators relevant for the electroweak fit.

Contents

1	Introduction	1
2	Standard Model fit	2
2.1	Experimental values of SM parameters	3
2.2	Theoretical expressions for EWPO	4
2.3	Experimental data for EWPO and fit results	7
3	Constraints on New Physics	12
3.1	Constraints on the oblique parameters	12
3.2	Constraints on the ϵ parameters	14
3.3	Constraints on the $Zb\bar{b}$ couplings	16
3.4	Constraints on a non-standard Higgs coupling	17
3.5	General bounds on the New Physics scale	20
4	Summary	24
A	NP contributions to the EW precision observables	24
B	Non-universal vertex corrections	26
C	Correlation matrices for fit results	27
D	Fit results for the observables with the large-m_t expansion for two-loop fermionic EW corrections to ρ_Z^f	32
E	Fit results for the observables using the full two-loop fermionic EW corrections to ρ_Z^f	35

1 Introduction

Electroweak Precision Observables (EWPO) have played a key role in constraining New Physics (NP) for the past twenty years [1–11]. The most striking examples of the power of these indirect constraints are the prediction of the top and Higgs masses. Concerning physics beyond the Standard Model (SM), the $\epsilon_{1,2,3,b}$ parameterization [6–8] allowed to extract interesting information without knowing the Higgs mass, although the constraining power of EWPO was somewhat diluted by the missing information on the Higgs boson and by the approximations necessary to write all LEP observables in terms of the $\epsilon_{1,2,3,b}$ parameters.

The experimental situation improved dramatically in the past year, with the precise measurement of the Higgs mass at the LHC [12–15]. In addition, the information on other key SM parameters such as the top and W boson masses has increased considerably, leading altogether to a sizable progress in the electroweak (EW) fit. It is therefore phenomenologically relevant to reassess the constraining power of the EW fit in the light of these recent experimental improvements. To this aim, we perform the EW fit in the SM and update the constraints on oblique NP and on modified $Zb\bar{b}$ couplings. Although the direct measurement of the Higgs boson mass completes the SM parameters relevant for the EW fit and thus makes the use of the $\epsilon_{1,2,3,b}$ parameters unnecessary, for the sake of comparison with previous analyses we will present also results for NP in this parameterization.

On the theory side, the full two-loop fermionic EW contributions to the R_b^0 observable have been recently numerically calculated in ref. [16]. The implementation of this result in the global fit has a large impact but represents a nontrivial problem, as we illustrate in detail below.

A very interesting question that can be tackled with present data is whether the Higgs boson is elementary or composite. Using a general effective Lagrangian for Higgs boson interactions [17–20], we analyze the constraints on the Higgs coupling to vector bosons, and find out that this coupling can be determined from the fit with an uncertainty of 5% at 95% probability, while much larger departures from the SM value are expected in generic composite Higgs models. Thus, the EW fit points to an elementary Higgs or to composite Higgs models in which additional contributions are present to restore the agreement with EWPO.

Finally, we consider the most general effective Lagrangian relevant for EWPO and compute the constraints on the coefficients of dimension six operators, which can be translated into lower bounds on the NP scale assuming a given value for the couplings.

To obtain our results, we perform a Bayesian analysis using the BAT library [21] and our own implementation of the EWPO formulæ. We have tested the agreement of our code with the ZFITTER (v6.43) one [22–25] and with outputs from the formulæ in refs. [26, 27].

The paper is organized as follows. In Section 2 we present the ingredients of the SM fit, the fitting procedure and the SM results. In Section 3.1 we present the results for the oblique parameters S , T and U . In Section 3.2 we discuss the results for $\epsilon_{1,2,3,b}$ parameters. In Section 3.3 we report the constraints on modified $Zb\bar{b}$ couplings. In Section 3.4 we present constraints on the Higgs coupling to vector bosons. In Section 3.5 we discuss the constraints on the effective Lagrangian relevant for EWPO and the bounds on the NP scale. Finally, in Section 4 we summarize our findings. Some technical details are presented in Appendices A and B, while more information on the fit results is reported in Appendices C, D and E.

2 Standard Model fit

The part of the SM Lagrangian relevant for the computation of EWPO can be defined in terms of the following free parameters: the fine structure constant α , the muon decay constant G_μ , the Z boson mass M_Z , the strong coupling $\alpha_s(M_Z^2)$, the top quark mass m_t

and the Higgs mass m_h . In addition, we introduce the effective parameter $\Delta\alpha_{\text{had}}^{(5)}(M_Z^2)$ to take into account the hadronic contribution to the running of α . In terms of the seven parameters above, the SM prediction for all other EWPO can be computed.¹

In the Bayesian approach we are following (see ref. [28] for details on the statistical treatment), prior distributions for the parameters α , G_μ , M_Z , $\alpha_s(M_Z^2)$, m_t , m_h and $\Delta\alpha_{\text{had}}^{(5)}(M_Z^2)$ have to be specified. However, given the very accurate experimental measurements of these parameters (see below), the results are insensitive to the choice of any reasonable prior.² The numerical results presented in the following are derived computing the region containing 68% of a marginalized probability distribution function (p.d.f.) starting from the mode and then symmetrizing the error, *i.e.*, the central value corresponds to the center of the 68% probability region and not to the mode. Since all p.d.f.'s obtained from the fit are almost gaussian, there is very little dependence on the prescription adopted.

2.1 Experimental values of SM parameters

The recent measurements of m_h by the ATLAS [12] and CMS [14] experiments are given by

$$m_h = \begin{cases} 125.5 \pm 0.2 \text{ (stat)}_{-0.6}^{+0.5} \text{ (syst) GeV} & \text{ATLAS,} \\ 125.7 \pm 0.3 \text{ (stat)} \pm 0.3 \text{ (syst) GeV} & \text{CMS.} \end{cases} \quad (2.1)$$

We adopt the average $m_h = 125.6 \pm 0.3$ GeV in the current study.³

According to ref. [29, 30], the world average of $\alpha_s(M_Z^2)$ from the fit to various data, excluding the EW precision measurements, is given by $\alpha_s(M_Z^2) = 0.1184 \pm 0.0006$.

For the hadronic contribution to the running of the electromagnetic coupling, we adopt the recent evaluation $\Delta\alpha_{\text{had}}^{(5)}(M_Z^2) = 0.02750 \pm 0.00033$ in ref. [31]. Note that other recent studies have reported much smaller uncertainties, e.g., $\Delta\alpha_{\text{had}}^{(5)}(M_Z^2) = 0.02757 \pm 0.00010$ [32], 0.027626 ± 0.000138 [33] and 0.027498 ± 0.000135 [34], where the first result relies on pQCD, and the last one has been derived with the Adler function approach. The result of ref. [33] differs from ref. [31] mainly in the use of exclusive (instead of inclusive) data in the range 1.2–2 GeV. Since exclusive determinations suffer from an unknown systematic uncertainty, we use the conservative result of ref. [31]. We prefer not to rely on the model-dependent results of refs. [32] and [34], although they are consistent with the values we are using.

In the absence of a world average for the top pole mass, we adopt the Tevatron average $m_t = 173.18 \pm 0.56 \text{ (stat)} \pm 0.75 \text{ (syst) GeV} = 173.2 \pm 0.9$ GeV [35], fully compatible with the LHC result $m_t = 173.3 \pm 0.5 \text{ (stat)} \pm 1.3 \text{ (syst) GeV}$ [36]. Since there might be subtleties related to the precise definition of the pole mass measured at Tevatron and LHC, we also use for comparison the determination of the $\overline{\text{MS}}$ mass $\overline{m}_t(\overline{m}_t) = 163.3 \pm 2.7$ GeV obtained

¹While they are negligible in most cases, we have kept all fermion masses whenever relevant. Furthermore, we have neglected fermion mixing.

²In practice, any reasonable prior, convoluted with the experimental measurement, will coincide with the experimental likelihood. Thus, we can use directly as prior for the above parameters their experimental gaussian likelihood.

³This naïve average might underestimate the error neglecting possible correlations in the systematics, however even doubling the error would not affect any of the results in this paper.

from the measurement of the $t\bar{t}$ production cross-section [37]. This value corresponds to $m_t = 173.3 \pm 2.8$ GeV.

For completeness, the other quark masses are taken to be $\bar{m}_u(2 \text{ GeV}) = 0.0023$ GeV, $\bar{m}_d(2 \text{ GeV}) = 0.0048$ GeV, $\bar{m}_s(2 \text{ GeV}) = 0.095$ GeV, $\bar{m}_c(\bar{m}_c) = 1.275$ GeV and $\bar{m}_b(\bar{m}_b) = 4.18$ GeV [29].

The renormalization group runnings of the strong coupling constant and the fermion masses are taken into account up to three-loop level [38–40].

The measurement of the Z boson mass is taken from LEP: $M_Z = 91.1875 \pm 0.0021$ GeV [41]. Finally, the parameters G_μ and α are fixed to be constants: $G_\mu = 1.1663787 \times 10^{-5}$ GeV⁻² and $\alpha = 1/137.035999074$, respectively [29].

2.2 Theoretical expressions for EWPO

The SM contributions to the EWPO have been calculated very precisely including higher-order radiative corrections. We adopt the on-mass-shell renormalization scheme [42–45], where the weak mixing angle is defined in terms of the physical masses of the gauge bosons:

$$s_W^2 \equiv \sin^2 \theta_W = 1 - \frac{M_W^2}{M_Z^2}, \quad (2.2)$$

and $c_W^2 = 1 - s_W^2$.

The Fermi constant G_μ in μ decay is taken as an input quantity instead of the W -boson mass, since the latter has not been measured very precisely compared to the former. The relation between G_μ and M_W is written as

$$G_\mu = \frac{\pi\alpha}{\sqrt{2}s_W^2 M_W^2} (1 + \Delta r), \quad (2.3)$$

where Δr represents radiative corrections. From eq. (2.3), the W -boson mass is calculated as

$$M_W^2 = \frac{M_Z^2}{2} \left(1 + \sqrt{1 - \frac{4\pi\alpha}{\sqrt{2}G_\mu M_Z^2} (1 + \Delta r)} \right). \quad (2.4)$$

The radiative corrections to Δr are known very precisely. In the current study, we employ the approximate formula for M_W , equivalently for Δr , in ref. [46], which includes the full one-loop EW corrections of $O(\alpha)$ [42, 43], the full two-loop QCD corrections of $O(\alpha\alpha_s)$ [47–53], three-loop QCD corrections of $O(G_\mu\alpha_s^2 m_t^2(1 + M_Z^2/m_t^2 + (M_Z^2/m_t^2)^2))$ [54–56], the full two-loop EW corrections of $O(\alpha^2)$ [46, 57–70], and leading three-loop corrections of $O(G_\mu^2\alpha_s m_t^4)$ and $O(G_\mu^3 m_t^6)$ [71, 72]. Further higher-order corrections are known to be negligibly small [73–78]. The remaining theoretical uncertainty in M_W coming from missing higher-order corrections is estimated to be 4 MeV [46]. Since this residual uncertainty is much smaller than the present experimental one, we do not take it into account.⁴ A comprehensive summary of the radiative corrections can be found in ref. [79].

⁴This uncertainty should however be added to the SM prediction quoted in table 3.

The interaction between the Z boson and the neutral current can be written in terms of the effective $Zf\bar{f}$ couplings g_V^f and g_A^f , of g_R^f and g_L^f , or of ρ_Z^f and κ_Z^f :

$$\mathcal{L} = \frac{e}{2s_W c_W} Z_\mu \sum_f \bar{f} \left(g_V^f \gamma_\mu - g_A^f \gamma_\mu \gamma_5 \right) f, \quad (2.5)$$

$$= \frac{e}{2s_W c_W} Z_\mu \sum_f \bar{f} \left[g_R^f \gamma_\mu (1 + \gamma_5) + g_L^f \gamma_\mu (1 - \gamma_5) \right] f, \quad (2.6)$$

$$= \frac{e}{2s_W c_W} \sqrt{\rho_Z^f} Z_\mu \sum_f \bar{f} \left[(I_3^f - 2Q_f \kappa_Z^f s_W^2) \gamma^\mu - I_3^f \gamma^\mu \gamma_5 \right] f, \quad (2.7)$$

where $e^2 = 4\pi\alpha$, Q_f is the electric charge of the fermion f and I_3^f is the third component of weak isospin. The effective mixing angle for a given fermion f is defined through the relation

$$\sin^2 \theta_{\text{eff}}^f = \text{Re}(\kappa_Z^f) s_W^2 = \frac{1}{4|Q_f|} \left[1 - \text{Re} \left(\frac{g_V^f}{g_A^f} \right) \right]. \quad (2.8)$$

The radiative corrections to the effective couplings and the weak mixing angle depend on the flavour of final-state fermions in general. The corrections to $\sin^2 \theta_{\text{eff}}^f$ are given in the forms of approximate formulæ [80–82], including the full two-loop EW corrections of $O(\alpha^2)$ as well as leading $O(G_\mu^2 \alpha_s m_t^4)$ and $O(G_\mu^3 m_t^6)$ corrections, where the bosonic two-loop EW contribution is still missing only in the $Z \rightarrow b\bar{b}$ channel. The theoretical uncertainty from missing higher-order corrections is estimated to be 4.7×10^{-5} for the leptonic channels [80, 81], and we neglect it in the following. We use those formulæ to calculate the coupling $\text{Re}(\kappa_Z^f)$ through eq. (2.8), while the imaginary part of $O(\alpha)$ is also included.

The complete two-loop formulæ for the coupling ρ_Z^f are currently missing. Recently, the complete fermionic two-loop EW corrections have been calculated for $R_b^0 = \Gamma_b/\Gamma_h$ in ref. [16], where an approximate formula has been presented. However, from this approximate formula alone we cannot extract the values of ρ_Z^f including fermionic two-loop corrections, that are necessary to compute other ρ_Z^f -dependent observables such as R_ℓ^0 , R_c^0 , Γ_Z and the hadronic cross section (see below for their definitions). The authors of ref. [16] have kindly provided us with the approximate formulæ for Γ_u/Γ_b and Γ_d/Γ_b [83], which allow us to use the experimental information on one more observable in addition to R_b^0 . To illustrate the impact of these two-loop corrections, we present our results for the SM fit in two scenarios. First, we use only the previously known leading and (where available) next-to-leading two-loop EW contributions of $O(G_\mu^2 m_t^4)$ and $O(G_\mu^2 m_t^2 M_Z^2)$ in the large- m_t expansion, together with the leading three-loop corrections of $O(G_\mu^2 \alpha_s m_t^4)$ and $O(G_\mu^3 m_t^6)$. Second, we use the approximate formulæ for Γ_u/Γ_b and Γ_d/Γ_b adding three free parameters to the fit, which represent the unknown corrections to ρ_Z^u , ρ_Z^d and ρ_Z^b . The corrections to $\rho_Z^{u,d}$ can then be determined using the formulæ for Γ_u/Γ_b and Γ_d/Γ_b . This is the optimal use we can make of the presently available theoretical information. It will be interesting to compare the fitted values of $\delta\rho_Z^u$, $\delta\rho_Z^d$ and $\delta\rho_Z^b$ with the theoretical expressions, once

these will be available. As we shall see below, the corrections computed in ref. [16, 83] are surprisingly large, so that an independent check of the computation would be very useful.

In the following, we consider so-called pseudo observables at the Z pole [84, 85], which are not directly measurable in experiments but can be extracted from real observables by subtracting initial-state QED corrections and a part of final-state QED/QCD corrections.

The asymmetry parameter \mathcal{A}_f for a channel $Z \rightarrow f\bar{f}$ is defined in terms of the effective couplings:

$$\mathcal{A}_f = \frac{2 \operatorname{Re} \left(g_V^f / g_A^f \right)}{1 + \left[\operatorname{Re} \left(g_V^f / g_A^f \right) \right]^2}. \quad (2.9)$$

The left-right asymmetry, the forward-backward asymmetry and the longitudinal polarization of the $\tau\bar{\tau}$ channel are written in terms of the asymmetry parameters:

$$A_{\text{LR}}^0 = \mathcal{A}_e, \quad (2.10)$$

$$A_{\text{FB}}^{0,f} = \frac{3}{4} \mathcal{A}_e \mathcal{A}_f, \quad (2.11)$$

$$P_\tau^{\text{pol}} = \mathcal{A}_\tau. \quad (2.12)$$

The partial width of Z decaying into a charged-lepton pair $\ell\bar{\ell}$, including contribution from final-state QED interactions, is given in terms of the effective couplings by [22, 79]:

$$\Gamma_\ell = \Gamma_0 |\rho_Z^f| \sqrt{1 - \frac{4m_\ell^2}{M_Z^2}} \left[\left(1 + \frac{2m_\ell^2}{M_Z^2} \right) \left(\left| \frac{g_V^\ell}{g_A^\ell} \right|^2 + 1 \right) - \frac{6m_\ell^2}{M_Z^2} \right] \left(1 + \frac{3}{4} \frac{\alpha(M_Z^2)}{\pi} Q_\ell^2 \right), \quad (2.13)$$

where $\Gamma_0 = G_\mu M_Z^3 / (24\sqrt{2}\pi)$ and m_ℓ is the mass of the final-state lepton. In the case of the $Z \rightarrow q\bar{q}$ channels, final-state QCD interactions have to be taken into account in addition to the QED ones:

$$\Gamma_q = N_c \Gamma_0 |\rho_Z^q| \left[\left| \frac{g_V^q}{g_A^q} \right|^2 R_V^q(M_Z^2) + R_A^q(M_Z^2) \right] + \Delta_{\text{EW/QCD}}, \quad (2.14)$$

where N_c is the color factor, and $R_V^q(s)$ and $R_A^q(s)$ are the so-called radiator factors for which we refer to refs. [22, 79, 86]. We add recent results for $O(\alpha_s^4)$ corrections [87] to the radiator functions. The last term $\Delta_{\text{EW/QCD}}$ denotes non-factorizable EW-QCD corrections [22, 88, 89]: $\Delta_{\text{EW/QCD}} = -0.113$ MeV for $q = u, c$, -0.160 MeV for $q = d, s$ and -0.040 MeV for $q = b$.⁵

The total decay width of the Z boson, denoted by Γ_Z , is then given by the sum of all possible channels:

$$\Gamma_Z = 3\Gamma_\nu + \Gamma_e + \Gamma_\mu + \Gamma_\tau + \Gamma_h, \quad (2.15)$$

where we have defined the hadronic width $\Gamma_h = \sum_q \Gamma_q$. Moreover the ratios of the widths

$$R_\ell^0 = \frac{\Gamma_h}{\Gamma_\ell}, \quad R_q^0 = \frac{\Gamma_q}{\Gamma_h}, \quad (2.16)$$

⁵The non-factorizable EW-QCD corrections have been neglected in the results of ref. [16, 83].

and the cross section for $e^+e^- \rightarrow Z \rightarrow \text{hadrons}$ at the Z pole

$$\sigma_h^0 = \frac{12\pi \Gamma_e \Gamma_h}{M_Z^2 \Gamma_Z^2} \quad (2.17)$$

are part of the EWPO.

For the W -boson decay width Γ_W , we use the one-loop formula in refs. [45, 79, 90].

2.3 Experimental data for EWPO and fit results

The latest Tevatron average of the W -boson mass is $M_W = 80.385 \pm 0.015$ GeV [91]. We use the results for Γ_Z , σ_h^0 , P_τ^{pol} , \mathcal{A}_f , $A_{\text{FB}}^{0,f}$ and R_f^0 from SLD/LEP-I [41, 84] and Γ_W from LEP-II/Tevatron [85]. All experimental inputs are summarized in the second column of table 1, where we take into account the correlations among the inputs that can be found in ref. [84].

In the third column of table 1 we present the results of the SM fit obtained using the top pole mass and the expressions for Γ_u/Γ_b and Γ_d/Γ_b from refs. [16, 83]. As discussed above, in this case we do not have enough information to compute Γ_Z , σ_h^0 and R_ℓ^0 at the same level of accuracy of R_b^0 and R_c^0 . We therefore add three free parameters to the fit, representing the fermionic two-loop corrections $\delta\rho_Z^u$, $\delta\rho_Z^\ell$ and $\delta\rho_Z^b$. These parameters affect only the observables Γ_Z , σ_h^0 and R_ℓ^0 , since we have

$$R_b^0 = \frac{\Gamma_b}{\Gamma_h} = \frac{1}{1 + 2 \left(\frac{\Gamma_u}{\Gamma_b} + \frac{\Gamma_d}{\Gamma_b} \right)}, \quad R_c^0 = \frac{\Gamma_c}{\Gamma_h} = \frac{\frac{\Gamma_u}{\Gamma_b}}{1 + 2 \left(\frac{\Gamma_u}{\Gamma_b} + \frac{\Gamma_d}{\Gamma_b} \right)}, \quad (2.18)$$

where we have used the approximation $\Gamma_u = \Gamma_c$ and $\Gamma_d = \Gamma_s$. In this way, while we cannot predict Γ_Z , σ_h^0 and R_ℓ^0 , we obtain a posterior for the parameters $\delta\rho_Z^u$, $\delta\rho_Z^\ell$ and $\delta\rho_Z^b$, which can be compared to the theoretical expressions once they become available. The other parameters $\delta\rho_Z^u$ and $\delta\rho_Z^d$ are determined from $\delta\rho_Z^b$ through Γ_u/Γ_b and Γ_d/Γ_b , respectively. Notice that fits performed using the formula for R_b^0 from ref. [16] and the formulæ for ρ_Z^f from ref. [63] are inconsistent, since the change in R_b^0 implies a change in $R_{c,\ell}^0$, Γ_Z and σ_h^0 . Furthermore, the results of ref. [16] imply much larger two-loop fermionic corrections than expected from the expansion in ref. [63]. In fact, we can estimate the size of the unknown two-loop corrections as follows:

$$\delta\rho_Z^q - \delta\rho_Z^b \approx \frac{\Gamma_q/\Gamma_b - \Gamma'_q/\Gamma'_b}{\Gamma'_q/\Gamma'_b} = \begin{cases} 4.8 \times 10^{-3} & \text{for } q = u, \\ 4.4 \times 10^{-3} & \text{for } q = d, \end{cases} \quad (2.19)$$

where Γ_f (Γ'_f) denotes a partial width including (omitting) the contribution from $\delta\rho_Z^f$, and the approximation $\rho_Z^f \approx 1$ has been used. Since these corrections are comparable in size to one-loop contributions, it would be desirable to have an independent confirmation of the calculation of ref. [16].

From the fit we also obtain posteriors for the SM parameters $\alpha_s(M_Z^2)$, $\Delta\alpha_{\text{had}}^{(5)}(M_Z^2)$, M_Z , m_t and m_h (see table 1). As can be seen in figure 1, while the posteriors are dominated

	Data	Fit	Indirect	Pull
$\alpha_s(M_Z^2)$	0.1184 ± 0.0006	0.1184 ± 0.0006	0.078 ± 0.024	-1.9
$\Delta\alpha_{\text{had}}^{(5)}(M_Z^2)$	0.02750 ± 0.00033	0.02742 ± 0.00026	0.02728 ± 0.00043	-0.4
M_Z [GeV]	91.1875 ± 0.0021	91.1878 ± 0.0021	91.204 ± 0.013	+1.2
m_t [GeV]	173.2 ± 0.9	173.5 ± 0.8	175.7 ± 2.6	+0.9
m_h [GeV]	125.6 ± 0.3	125.6 ± 0.3	98.5 ± 27.7	-0.8
$\delta\rho_Z^\nu$	—	-0.0052 ± 0.0031	—	—
$\delta\rho_Z^\ell$	—	-0.0002 ± 0.0010	—	—
$\delta\rho_Z^b$	—	-0.0021 ± 0.0011	—	—
$\delta\rho_Z^u$	—	0.0026 ± 0.0012	—	—
$\delta\rho_Z^d$	—	0.0023 ± 0.0012	—	—
M_W [GeV]	80.385 ± 0.015	80.366 ± 0.007	80.361 ± 0.007	-1.4
Γ_W [GeV]	2.085 ± 0.042	2.0890 ± 0.0006	2.0890 ± 0.0006	+0.1
Γ_Z [GeV]	2.4952 ± 0.0023	2.4952 ± 0.0023	—	—
σ_h^0 [nb]	41.540 ± 0.037	41.539 ± 0.037	—	—
$\sin^2\theta_{\text{eff}}^{\text{lept}}(Q_{\text{FB}}^{\text{had}})$	0.2324 ± 0.0012	0.23145 ± 0.00009	0.23145 ± 0.00009	-0.8
P_τ^{pol}	0.1465 ± 0.0033	0.1476 ± 0.0007	0.1476 ± 0.0007	+0.3
\mathcal{A}_ℓ (SLD)	0.1513 ± 0.0021	0.1476 ± 0.0007	0.1470 ± 0.0008	-1.9
\mathcal{A}_c	0.670 ± 0.027	0.6681 ± 0.0003	0.6681 ± 0.0003	-0.1
\mathcal{A}_b	0.923 ± 0.020	0.93466 ± 0.00006	0.93466 ± 0.00006	+0.6
$A_{\text{FB}}^{0,\ell}$	0.0171 ± 0.0010	0.0163 ± 0.0002	0.0163 ± 0.0002	-0.8
$A_{\text{FB}}^{0,c}$	0.0707 ± 0.0035	0.0739 ± 0.0004	0.0740 ± 0.0004	+0.9
$A_{\text{FB}}^{0,b}$	0.0992 ± 0.0016	0.1034 ± 0.0005	0.1038 ± 0.0005	+2.7
R_ℓ^0	20.767 ± 0.025	20.768 ± 0.025	—	—
R_c^0	0.1721 ± 0.0030	0.17247 ± 0.00002	0.17247 ± 0.00002	+0.1
R_b^0	0.21629 ± 0.00066	0.21492 ± 0.00003	0.21492 ± 0.00003	-2.1

Table 1. Summary of experimental data and fit results in the SM, including the subleading two-loop fermionic EW corrections to ρ_Z^f with the results of ref. [16, 83] and introducing the parameters $\delta\rho_Z^{\nu,\ell,b}$. The values in the column “Indirect” are determined without using the corresponding experimental information. The last column shows the pulls in units of standard deviations evaluated from the p.d.f.’s of “Data” and “Indirect” as explained in ref. [92]. For completeness we also report the fit result for $\delta\rho_Z^{u,d}$ computed from $\delta\rho_Z^b$ using $\Gamma_{u,d}/\Gamma_b$.

by the experimental input (as desirable for fit input parameters), the fit would provide an indirect determination with a compatible result and a remarkable accuracy (with the well-known exception of the Higgs mass which is poorly indirectly determined).⁶ The correlation matrix for the posteriors is given in table 11.

To show the impact on the fit of the new calculation of R_b^0 [16], we present in table 2 the results obtained using instead refs. [57–63] for the leading and next-to-leading terms in

⁶Actually the indirect determination of $\alpha_s(M_Z^2)$ is not very precise when we use the results of ref. [16], due to the uncertainty related to $\delta\rho_Z^\nu$, $\delta\rho_Z^\ell$ and $\delta\rho_Z^b$. This can be seen by comparing the first and the next-to-last plots in figure 1.

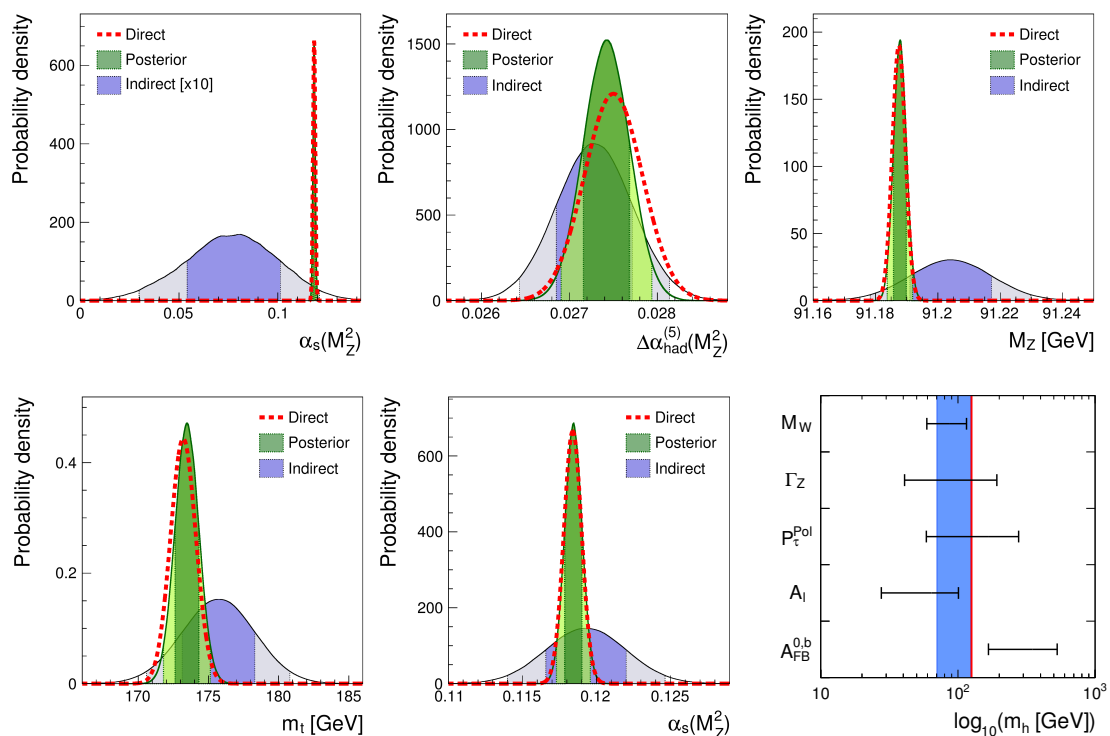


Figure 1. Comparisons between the direct measurement and the posterior probability distributions for the input parameters in the SM fit, together with their indirect determinations from the EWPO measurements, obtained by assuming a flat prior for the single parameter under consideration. Using the results of ref. [16, 83] and introducing the parameters $\delta\rho_Z^{\nu,\ell,b}$, the subleading two-loop fermionic EW corrections to ρ_Z^f have been taken into account in the plots, except for the bottom-center and bottom-right plots, in which the corrections have been omitted. Here and in the following, the dark (light) regions correspond to 68% (95%) probability. In the bottom-right plot, we report the indirect determinations of the Higgs mass excluding the observables M_W , Γ_Z , P_τ^{Pol} , \mathcal{A}_l and $A_{\text{FB}}^{0,b}$, except for the one specified in each row. The vertical blue (red) band represents the one obtained from the fit with all the observables (from the direct measurement). We assume a flat prior for the Higgs mass ranging from 10 MeV to 1 TeV.

the large- m_t expansion for two-loop fermionic EW corrections to ρ_Z^f . The corresponding correlation matrix for the posteriors is given in table 12. As can be seen by comparing with the full results, the tension in R_b^0 is reduced. The predictions for EWPO are reported in table 3. Notice that the indirect determination of $\alpha_s(M_Z^2)$ is much more precise in this case since we are not considering large unknown fermionic corrections to ρ_Z^f (see the bottom center plot in figure 1).

Using as SM input $m_t = 173.3 \pm 2.8$ GeV obtained from the $\overline{\text{MS}}$ mass instead of the Tevatron pole mass average, one obtains the posterior $m_t = 174.6 \pm 1.9$ (174.9 ± 1.9) GeV using the results of ref. [16, 83] (using the large- m_t expansion), on the upper end of the Tevatron result. Concerning the EWPO fit, the main observables affected by the change in m_t are M_W , Γ_W and R_b^0 , for which we obtain $M_W = 80.371 \pm 0.011$ (80.373 ± 0.010) GeV,

	Data	Fit	Indirect	Pull
$\alpha_s(M_Z^2)$	0.1184 ± 0.0006	0.1184 ± 0.0006	0.1193 ± 0.0027	+0.3
$\Delta\alpha_{\text{had}}^{(5)}(M_Z^2)$	0.02750 ± 0.00033	0.02740 ± 0.00026	0.02725 ± 0.00042	-0.5
M_Z [GeV]	91.1875 ± 0.0021	91.1878 ± 0.0021	91.197 ± 0.012	+0.8
m_t [GeV]	173.2 ± 0.9	173.5 ± 0.8	176.3 ± 2.5	+1.1
m_h [GeV]	125.6 ± 0.3	125.6 ± 0.3	97.3 ± 26.9	-0.9
M_W [GeV]	80.385 ± 0.015	80.367 ± 0.007	80.362 ± 0.007	-1.4
Γ_W [GeV]	2.085 ± 0.042	2.0891 ± 0.0006	2.0891 ± 0.0006	+0.1
Γ_Z [GeV]	2.4952 ± 0.0023	2.4953 ± 0.0004	2.4953 ± 0.0004	+0.0
σ_h^0 [nb]	41.540 ± 0.037	41.484 ± 0.004	41.484 ± 0.004	-1.5
$\sin^2 \theta_{\text{eff}}^{\text{lept}}(Q_{\text{FB}}^{\text{had}})$	0.2324 ± 0.0012	0.23145 ± 0.00009	0.23144 ± 0.00009	-0.8
P_τ^{pol}	0.1465 ± 0.0033	0.1476 ± 0.0007	0.1477 ± 0.0007	+0.3
\mathcal{A}_ℓ (SLD)	0.1513 ± 0.0021	0.1476 ± 0.0007	0.1471 ± 0.0008	-1.9
\mathcal{A}_c	0.670 ± 0.027	0.6682 ± 0.0003	0.6682 ± 0.0003	-0.1
\mathcal{A}_b	0.923 ± 0.020	0.93466 ± 0.00006	0.93466 ± 0.00006	+0.6
$A_{\text{FB}}^{0,\ell}$	0.0171 ± 0.0010	0.0163 ± 0.0002	0.0163 ± 0.0002	-0.8
$A_{\text{FB}}^{0,c}$	0.0707 ± 0.0035	0.0740 ± 0.0004	0.0740 ± 0.0004	+0.9
$A_{\text{FB}}^{0,b}$	0.0992 ± 0.0016	0.1035 ± 0.0005	0.1039 ± 0.0005	+2.8
R_ℓ^0	20.767 ± 0.025	20.735 ± 0.004	20.734 ± 0.004	-1.3
R_c^0	0.1721 ± 0.0030	0.17223 ± 0.00002	0.17223 ± 0.00002	+0.0
R_b^0	0.21629 ± 0.00066	0.21575 ± 0.00003	0.21575 ± 0.00003	-0.8

Table 2. Same as table 1, but using the large- m_t expansion for the two-loop fermionic EW corrections to ρ_Z^f .

$\Gamma_W = 2.0894 \pm 0.0009$ (2.0896 ± 0.0008) GeV and $R_b^0 = 0.21488 \pm 0.00007$ (0.21570 ± 0.00007).

Let us now discuss the compatibility of the SM prediction with experimental data. To this aim, we use the compatibility plots introduced in ref. [92], where the difference in standard deviations between the fit prediction and the experimental result is given by the color coding.

The compatibility of M_W , \mathcal{A}_ℓ and $A_{\text{FB}}^{0,b}$ is shown in figure 2. While these results are stable against the inclusion of the recently calculated two-loop fermionic corrections to R_b^0 , the compatibility of R_b^0 is worsened by the inclusion of the results in ref. [16], as can be seen by comparing the plots in figure 3.

In the bottom-right plot in figure 1 we report the indirect determinations of the Higgs mass obtained considering the constraints from M_W , Γ_Z , P_τ^{pol} , A_ℓ^0 and $A_{\text{FB}}^{0,b}$ one at a time, as well as the full fit result and the direct measurement, omitting the results of ref. [16].

Our numerical results agree with those obtained using the ZFITTER package [22–25]. Our fit results are compatible with the ones obtained by the LEP Electroweak Working Group [85] and also with the ones in refs. [93, 94]. A comparison with the recent Gfitter group fits [95, 96] is not straightforward since the result for R_b^0 of ref. [16] has been used without correspondingly modifying other Γ_q -related observables and without accounting for other possibly large fermionic two-loop corrections.

	Prediction	α_s	$\Delta\alpha_{\text{had}}^{(5)}$	M_Z	m_t
M_W [GeV]	80.362 ± 0.008	± 0.000	± 0.006	± 0.003	± 0.005
Γ_W [GeV]	2.0888 ± 0.0007	± 0.0002	± 0.0005	± 0.0002	± 0.0004
Γ_Z [GeV]	2.4951 ± 0.0005	± 0.0003	± 0.0003	± 0.0002	± 0.0002
σ_h^0 [nb]	41.484 ± 0.004	± 0.003	± 0.000	± 0.002	± 0.001
$\sin^2 \theta_{\text{eff}}^{\text{lept}}(Q_{\text{FB}}^{\text{had}})$	0.23149 ± 0.00012	± 0.00000	± 0.00012	± 0.00001	± 0.00003
$P_7^{\text{pol}} = \mathcal{A}_\ell$	0.1472 ± 0.0009	± 0.0000	± 0.0009	± 0.0001	± 0.0002
\mathcal{A}_c	0.6680 ± 0.0004	± 0.0000	± 0.0004	± 0.0001	± 0.0001
\mathcal{A}_b	0.93464 ± 0.00008	± 0.00000	± 0.00007	± 0.00001	± 0.00001
$A_{\text{FB}}^{0,\ell}$	0.0163 ± 0.0002	± 0.0000	± 0.0002	± 0.0000	± 0.0000
$A_{\text{FB}}^{0,c}$	0.0738 ± 0.0005	± 0.0000	± 0.0005	± 0.0001	± 0.0001
$A_{\text{FB}}^{0,b}$	0.1032 ± 0.0007	± 0.0000	± 0.0006	± 0.0001	± 0.0002
R_ℓ^0	20.734 ± 0.004	± 0.004	± 0.002	± 0.000	± 0.000
R_c^0	0.17222 ± 0.00002	± 0.00001	± 0.00001	± 0.00000	± 0.00001
R_b^0	0.21576 ± 0.00003	± 0.00000	± 0.00000	± 0.00001	± 0.00003
R_c^0	0.17247 ± 0.00002	± 0.00001	± 0.00001	± 0.00000	± 0.00001
R_b^0	0.21493 ± 0.00004	± 0.00001	± 0.00000	± 0.00000	± 0.00003

Table 3. SM predictions computed using the theoretical expressions for EWPO without the experimental constraints on the observables, and individual uncertainties associated with each input parameter: $\alpha_s(M_Z^2) = 0.1184 \pm 0.0006$, $\Delta\alpha_{\text{had}}^{(5)}(M_Z^2) = 0.02750 \pm 0.00033$, $M_Z = 91.1875 \pm 0.0021$ GeV and $m_t = 173.2 \pm 0.9$ GeV, where the uncertainty associated to $m_h = 125.6 \pm 0.3$ GeV is always negligible. The predictions are computed with the large- m_t expansion for the two-loop fermionic EW corrections to ρ_Z^f , except for R_c^0 and R_b^0 in the last two rows, which are computed with the results of ref. [16, 83].

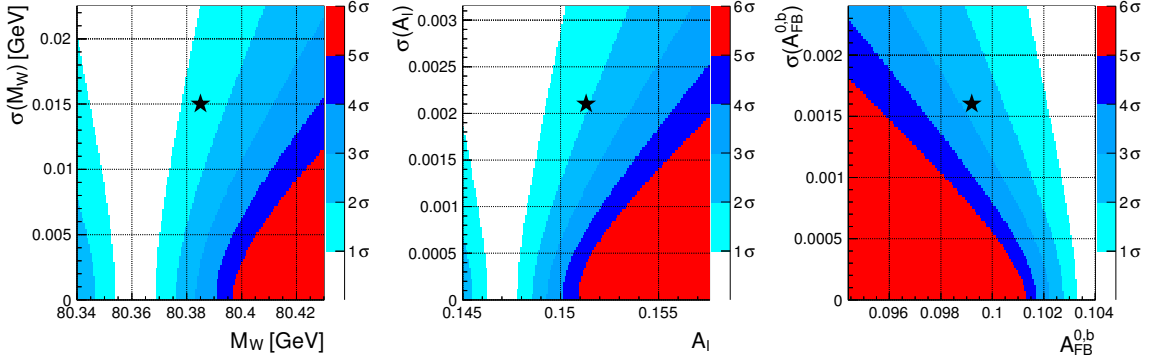


Figure 2. Compatibility plots of M_W , \mathcal{A}_ℓ and $A_{\text{FB}}^{0,b}$. Any direct measurement corresponds to a point in the (central value, experimental error) plane, and its compatibility with the indirect determination is given in numbers of standard deviations by the color coding. The present experimental result is indicated by a star.

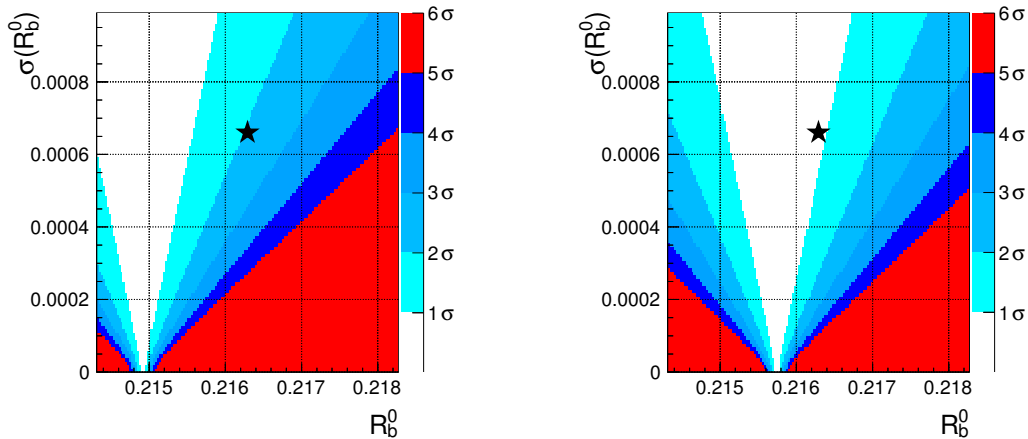


Figure 3. Compatibility plot of R_b^0 computed using the results of ref. [16] (left) or the large m_t expansion for the two-loop fermionic EW corrections to ρ_Z^f (right).

3 Constraints on New Physics

Let us now discuss the EW fit beyond the SM, using several widely adopted model-independent parameterizations of NP contributions. Before dwelling into the details of the different analyses, a discussion on the inclusion of the results of ref. [16, 83] is mandatory. In our SM fit (see Section 2), we parameterized the unknown two-loop fermionic EW corrections to ρ_Z^f with three free parameters. The fit result selects values of these corrections that are as large as the ones computed by Freitas and Huang, and much larger than naively expected from the large- m_t expansion. Waiting for a complete calculation of these corrections, we cannot use consistently the results of ref. [16, 83] in NP fits where the use of R_ℓ^0 , Γ_Z and σ_h^0 is necessary to constrain NP contributions. Thus, in these cases we only present results obtained using the large- m_t expansion for the two-loop fermionic EW corrections to ρ_Z^f , while in other cases we present results using both the large- m_t expansion and the expressions in ref. [16, 83], leaving the choice of the preferred option to the reader. In the latter case, we do not use the observables Γ_Z , R_ℓ^0 and R_c^0 in the fit. In all the NP fits reported below, the fit result for SM parameters practically coincides with the input reported in table 1.

3.1 Constraints on the oblique parameters

In several NP scenarios, the dominant NP effects appear in the gauge-boson vacuum-polarization corrections, called oblique corrections [97, 98]. If the NP scale is sufficiently higher than the weak scale, the oblique corrections are effectively described by the three independent parameters S , T and U [4, 99]:

$$S = -16\pi\Pi_{30}^{\text{NP}'}(0) = 16\pi [\Pi_{33}^{\text{NP}'}(0) - \Pi_{3Q}^{\text{NP}'}(0)], \quad (3.1)$$

$$T = \frac{4\pi}{s_W^2 c_W^2 M_Z^2} [\Pi_{11}^{\text{NP}}(0) - \Pi_{33}^{\text{NP}}(0)], \quad (3.2)$$

Parameter	Large- m_t expansion		Using ref. [16, 83]
	STU fit	ST fit with $U = 0$	ST fit with $U = 0$
S	0.04 ± 0.10	0.06 ± 0.09	0.08 ± 0.10
T	0.05 ± 0.12	0.08 ± 0.07	0.10 ± 0.08
U	0.03 ± 0.09	—	—

Table 4. Fit results for the oblique parameters with floating U or fixing $U = 0$, using the large- m_t expansion or with the results of ref. [16, 83] for the two-loop fermionic EW corrections to ρ_Z^f . In the latter case, we do not consider constraints from Γ_Z , σ_h^0 and R_ℓ^0 .

$$U = 16\pi [\Pi_{11}^{\text{NP}'}(0) - \Pi_{33}^{\text{NP}'}(0)], \quad (3.3)$$

where Π_{XY}^{NP} with $X, Y = 0, 1, 3, Q$ denotes NP contribution to the vacuum polarization amplitude of the gauge bosons defined, e.g., in ref. [4], $\Pi'_{XY}(q^2) = d\Pi_{XY}(q^2)/dq^2$, and s_W^2 and c_W^2 represent their SM values. NP contributions to an observable, parameterized by the above oblique parameters, add up to the SM contribution:

$$\mathcal{O} = \mathcal{O}_{\text{SM}} + \mathcal{O}_{\text{NP}}(S, T, U), \quad (3.4)$$

where $S = T = U = 0$ in the SM, and we linearize the NP contribution in terms of the oblique parameters [4, 99–102]. Explicit formulæ for the observables are summarized in Appendix A. Actually, all EWPO can be expressed in terms of the following combinations of oblique parameters:

$$\begin{aligned} A &= S - 2c_W^2 T - \frac{(c_W^2 - s_W^2)U}{2s_W^2}, \\ B &= S - 4c_W^2 s_W^2 T, \\ C &= -10(3 - 8s_W^2)S + (63 - 126s_W^2 - 40s_W^4)T. \end{aligned} \quad (3.5)$$

Note that the parameter C describes the NP contribution to Γ_Z , the parameter A (the only one containing U) describes the NP contribution to M_W and Γ_W , and NP contributions to all other EWPO are proportional to B . Clearly, for S, T and U all different from zero, Γ_Z is necessary to obtain bounds on the NP parameters, so in this case we only use the large- m_t expansion. We fit the three oblique parameters together with the SM parameters to the EW precision data in table 1. The fit results are summarized in the second column of table 4, and the correlation matrix is given in table 13. The two-dimensional probability distribution for S and T is shown in the left plot of figure 4.

If one fixes $U = 0$, which is the case in many NP models where $U \ll S, T$, the fit yields the results in the third (fourth) column of table 4, with correlation matrices given in table 14 (15) omitting (using) the formulæ of ref. [16, 83]. The corresponding two-dimensional distribution is given in the center and right plots in figure 4. As expected, the results in the case $U = 0$ do not depend sizably on the choice made for the two-loop fermionic EW corrections.

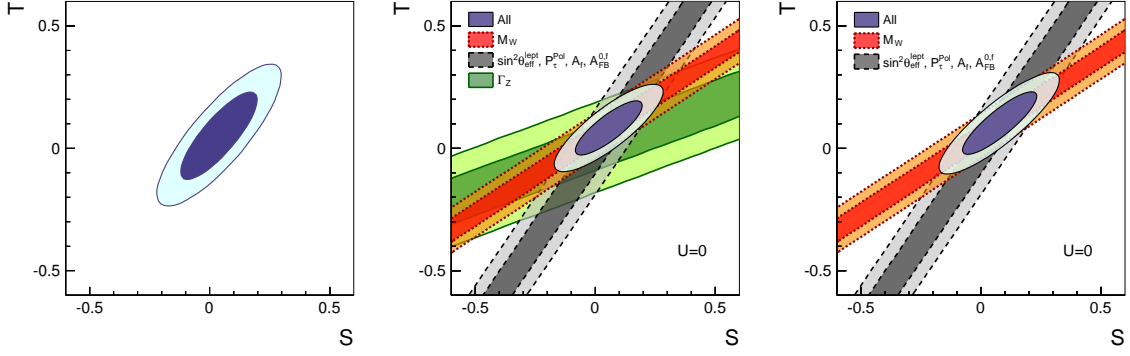


Figure 4. Left: Two-dimensional probability distribution for the oblique parameters S and T obtained from the fit with S , T , U and the SM parameters, with the large- m_t expansion for the two-loop fermionic EW corrections to ρ_Z^f . Center: Two-dimensional probability distribution for the oblique parameters S and T obtained from the fit with S , T and the SM parameters with $U = 0$, with the large- m_t expansion for the two-loop fermionic EW corrections to ρ_Z^f . The individual constraints from M_W , the asymmetry parameters $\sin^2 \theta_{\text{eff}}^{\text{left}}$, P_τ^{pol} , A_f and $A_{\text{FB}}^{0,f}$ with $f = \ell, c, b$, and Γ_Z are also presented, corresponding to the combinations of parameters A , B and C in eq. (3.5). Right: Same as center, but using the results of ref. [16, 83]. In this case, the constraint from Γ_Z cannot be used.

3.2 Constraints on the ϵ parameters

Aiming at a fully model-independent analysis of EWPO in the absence of experimental information on the Higgs sector, Altarelli and Barbieri introduced the parameters ϵ_1 , ϵ_2 and ϵ_3 [6, 7]:

$$\epsilon_1 = \Delta\rho', \quad (3.6)$$

$$\epsilon_2 = c_0^2 \Delta\rho' + \frac{s_0^2}{c_0^2 - s_0^2} \Delta r_W - 2s_0^2 \Delta\kappa', \quad (3.7)$$

$$\epsilon_3 = c_0^2 \Delta\rho' + (c_0^2 - s_0^2) \Delta\kappa', \quad (3.8)$$

where Δr_W , $\Delta\rho'$ and $\Delta\kappa'$ are defined through the relations

$$s_W^2 c_W^2 = \frac{\pi\alpha(M_Z^2)}{\sqrt{2}G_\mu M_Z^2(1 - \Delta r_W)}, \quad (3.9)$$

$$\sqrt{\text{Re} \rho_Z^e} = 1 + \frac{\Delta\rho'}{2}, \quad (3.10)$$

$$\sin^2 \theta_{\text{eff}}^e = (1 + \Delta\kappa') s_0^2 \quad (3.11)$$

with

$$s_0^2 c_0^2 = \frac{\pi\alpha(M_Z^2)}{\sqrt{2}G_\mu M_Z^2}, \quad (3.12)$$

and $c_0^2 = 1 - s_0^2$. Unlike the oblique parameters S , T and U discussed in Section 3.1, the ϵ parameters include the SM contribution in addition to possible NP contributions. Moreover, they involve not only oblique corrections, but also vertex corrections. The

Parameter	Large- m_t expansion	
	$\epsilon_{1,2,3,b}$ fit	$\epsilon_{1,3}$ fit
$\epsilon_1 [10^{-3}]$	5.6 ± 1.0	6.0 ± 0.6
$\epsilon_2 [10^{-3}]$	-7.8 ± 0.9	—
$\epsilon_3 [10^{-3}]$	5.6 ± 0.9	5.9 ± 0.8
$\epsilon_b [10^{-3}]$	-5.8 ± 1.3	—

Table 5. Fit results for the ϵ parameters, with floating $\epsilon_{1,2,3,b}$, or with assuming $\epsilon_2 = \epsilon_2^{\text{SM}}$ and $\epsilon_b = \epsilon_b^{\text{SM}}$. The non-universal vertex corrections and the SM values for the ϵ parameters are computed with the large- m_t expansion for the two-loop fermionic EW corrections to ρ_Z^f .

ϵ parameters are defined in such a way that the logarithmic corrections are separated from the large quadratic corrections proportional to the top-quark mass. The quadratic corrections are then parameterized by ϵ_1 , while the other corrections are included in ϵ_2 and ϵ_3 .

In the SM, the $Z \rightarrow b\bar{b}$ vertex receives large corrections from the top-quark loop, which can be parametrized by an additional parameter ϵ_b [8]. However, given the present experimental accuracy on EWPO, the flavour non-universal vertex corrections in the SM have to be taken into account in all channels. We define

$$\begin{aligned}\rho_Z^f &= \rho_Z^e + \Delta\rho_Z^f, \\ \kappa_Z^f &= \kappa_Z^e + \Delta\kappa_Z^f\end{aligned}\tag{3.13}$$

for $f \neq b$, and

$$\begin{aligned}\rho_Z^b &= \left(\rho_Z^e + \Delta\rho_Z^b\right) (1 + \epsilon_b)^2, \\ \kappa_Z^b &= \frac{\kappa_Z^e + \Delta\kappa_Z^b}{1 + \epsilon_b},\end{aligned}\tag{3.14}$$

where the non-universal corrections $\Delta\rho_Z^f$ and $\Delta\kappa_Z^f$ are defined in Appendix B. In refs. [103, 104], the relations between the observables and the ϵ parameters are linearized. However, in the case of the W -boson mass, the difference between the values derived with and without the linearization is comparable in size to the current experimental uncertainty. Therefore, we do not employ any linearization in our analysis.

We fit the four ϵ parameters together with the SM parameters to the precision observables listed in table 1, except for Γ_W , which is not directly related to ϵ 's. The fit results are given in the second column of table 5, and the corresponding correlation matrix is summarized in table 16. Fixing $\epsilon_2 = \epsilon_2^{\text{SM}}$ and $\epsilon_b = \epsilon_b^{\text{SM}}$ in the fit, we obtain the results in the third column of table 5 with the correlation matrix in table 17. The two-dimensional probability distributions for ϵ_1 and ϵ_3 in both fits are shown in figure 5, where in the case of $\epsilon_2 = \epsilon_2^{\text{SM}}$ and $\epsilon_b = \epsilon_b^{\text{SM}}$ we also plot the individual constraints. To show the impact of including non-universal vertex corrections, we also report in figure 5 the probability regions obtained omitting these terms.

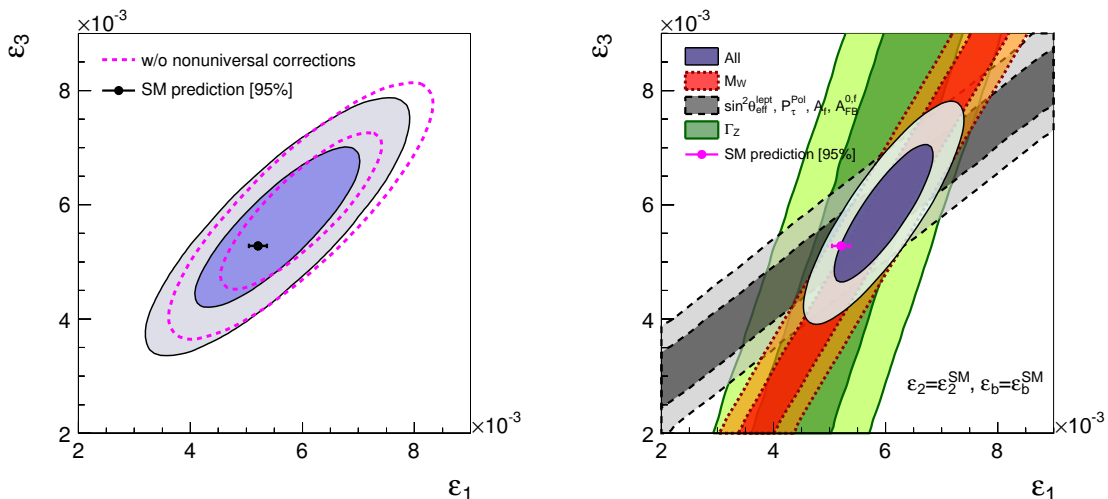


Figure 5. Two-dimensional probability distributions for ϵ_1 and ϵ_3 in the fit, with floating $\epsilon_{1,2,3,b}$ (left), or with assuming $\epsilon_2 = \epsilon_2^{\text{SM}}$ and $\epsilon_b = \epsilon_b^{\text{SM}}$ (right). In the left plot, the effect of non-universal vertex corrections is presented. In the right plot, we also show the impact of different constraints. The SM prediction at 95% is denoted by a point with an error bar.

The corresponding SM predictions for the ϵ parameters with the large- m_t expansion for the two-loop fermionic EW corrections to ρ_Z^f are given by:

$$\begin{aligned}
\epsilon_1^{\text{SM}} &= (5.21 \pm 0.08) 10^{-3} \quad ([5.04, 5.37] 10^{-3} \text{ @95\% prob.}), \\
\epsilon_2^{\text{SM}} &= -(7.37 \pm 0.03) 10^{-3} \quad ([-7.43, -7.32] 10^{-3} \text{ @95\% prob.}), \\
\epsilon_3^{\text{SM}} &= (5.279 \pm 0.004) 10^{-3} \quad ([5.271, 5.288] 10^{-3} \text{ @95\% prob.}), \\
\epsilon_b^{\text{SM}} &= -(6.94 \pm 0.15) 10^{-3} \quad ([-7.24, -6.64] 10^{-3} \text{ @95\% prob.}), \quad (3.15)
\end{aligned}$$

where the uncertainties are dominated by the top-quark mass, and the quadratic dependence in ϵ_1^{SM} and ϵ_b^{SM} results in the larger uncertainties. The 95% ranges of ϵ_1^{SM} and ϵ_b^{SM} become $[4.71, 5.72] 10^{-3}$ and $[-7.49, -6.41] 10^{-3}$, respectively, if adopting $m_t = 173.3 \pm 2.8$ GeV instead of $m_t = 173.2 \pm 0.9$ GeV. Notice that one can define ϵ_b^{SM} either from the first or from the second of eq. (3.14). We choose to define it from κ_Z^b , so that the prediction is insensitive to the inclusion of two-loop fermionic contributions to ρ_Z^b (this is possible within the approximations inherent in the ϵ parameterization). In figure 5 we report the one-dimensional 95% probability range of the SM predictions for ϵ_1 and ϵ_3 , where the latter is invisible due to the tiny error band.

3.3 Constraints on the $Zb\bar{b}$ couplings

Motivated phenomenologically by the long-standing pull in $A_{\text{FB}}^{0,b}$ and by the more recent pull in R_b^0 , and theoretically by the larger coupling to NP in the third generation realized in many explicit models, the possibility of modified $Zb\bar{b}$ couplings has been extensively studied (see for example refs. [105–118]).

Parameter	Large- m_t expansion	Using ref. [16, 83]
δg_R^b	0.018 ± 0.007	0.019 ± 0.007
δg_L^b	0.0028 ± 0.0014	0.0016 ± 0.0015
δg_V^b	0.021 ± 0.008	0.020 ± 0.008
δg_A^b	-0.015 ± 0.006	-0.017 ± 0.006

Table 6. Fit results for the shifts in the $Zb\bar{b}$ couplings, using the large- m_t expansion or the results in ref. [16, 83] for the two-loop fermionic two-loop EW corrections. In the latter case, we do not consider constraints from Γ_Z , σ_h^0 and R_ℓ^0 .

We parameterize NP contributions to the $Zb\bar{b}$ vertex by modifying the couplings in eq. (2.5) in the following way:

$$g_V^b = (g_V^b)_{\text{SM}} + \delta g_V^b, \quad g_A^b = (g_A^b)_{\text{SM}} + \delta g_A^b, \quad (3.16)$$

or equivalently by introducing $\delta g_R^b = (\delta g_V^b - \delta g_A^b)/2$ and $\delta g_L^b = (\delta g_V^b + \delta g_A^b)/2$. We may assume flat priors either for δg_V^b and δg_A^b or for δg_R^b and δg_L^b , but both choices yield almost identical results. Here we perform a fit with flat priors for δg_R^b and δg_L^b . The results are summarized in table 6, where the correlation matrices for the posteriors are given in tables 18 and 19. There is also a second region in the fit (not shown in table 6 nor in figure 6) where g_R flips its sign.⁷

As shown in the left plots in figure 6, the asymmetries \mathcal{A}_b and $A_{\text{FB}}^{0,b}$ are mainly sensitive to δg_R^b , since their shifts are given in terms of the combination $(g_L^b)_{\text{SM}}\delta g_R^b - (g_R^b)_{\text{SM}}\delta g_L^b$ with $|(g_R^b)_{\text{SM}}| \ll |(g_L^b)_{\text{SM}}|$. On the other hand, R_b^0 is associated with $(g_R^b)_{\text{SM}}\delta g_R^b + (g_L^b)_{\text{SM}}\delta g_L^b$, and mainly constrains δg_L^b .

3.4 Constraints on a non-standard Higgs coupling

A key question to understand the mechanism of EWSB is whether the underlying dynamics is weak or strong. As we shall see below, EWPO strongly constrain the Higgs coupling to vector bosons, and this hints either at a weakly interacting Higgs or at a non-trivial strongly interacting sector in which additional contributions to EWPO are present and restore the agreement with experimental data.

To investigate the question above, it is useful to consider a general Lagrangian for a light Higgs-like scalar field h [17–20]. Under the assumption of an approximate custodial symmetry, the longitudinal W and Z polarizations can be described by the two-by-two matrix $\Sigma(x) = \exp(i\tau^a \chi^a(x)/v)$, with τ^a the Pauli matrices and $v^2 = 1/(\sqrt{2}G_\mu)$. Then, assuming that there are no other light states and no new sources of flavour violation, the most general Lagrangian for h can be written as [18, 19]:

$$\begin{aligned} \mathcal{L} = & \frac{1}{2}(\partial_\mu h)^2 - V(h) + \frac{v^2}{4} \text{Tr}(D_\mu \Sigma^\dagger D^\mu \Sigma) \left(1 + 2a \frac{h}{v} + b \frac{h^2}{v^2} + \dots \right) \\ & - m_{u,i}(\bar{u}_{L,i}, \bar{d}_{L,i}) \Sigma \begin{pmatrix} u_{R,i} \\ 0 \end{pmatrix} \left(1 + c_u \frac{h}{v} + c_{2u} \frac{h^2}{v^2} + \dots \right) + \text{h.c.} \end{aligned}$$

⁷The other two allowed regions from the EWPO fit are disfavored by the off Z -pole data [107].

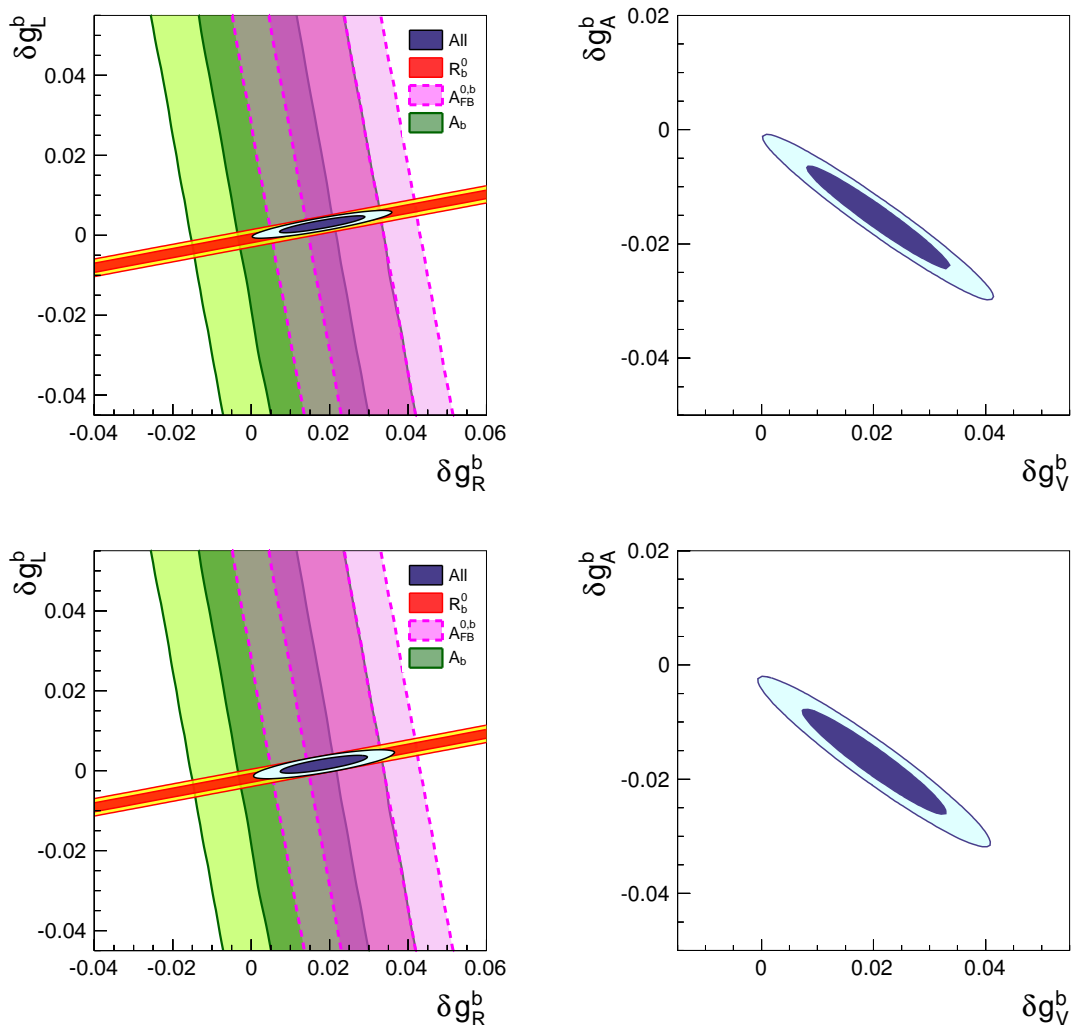


Figure 6. Two-dimensional probability distributions for the parameters δg_R^b and δg_L^b (left), or δg_V^b and δg_A^b (right), using the large- m_t expansion (top) or the results of ref. [16, 83] (bottom) for the two-loop fermionic EW corrections to ρ_Z^f . The individual constraints in the left plots are computed by omitting \mathcal{A}_b , $A_{\text{FB}}^{0,b}$, Γ_Z , σ_h^0 , R_ℓ^0 , R_c^0 and R_b^0 except for the one specified in the legend.

$$\begin{aligned}
& -m_{d,i}(\bar{u}_{L,i}, \bar{d}_{L,i}) \Sigma \begin{pmatrix} 0 \\ d_{R,i} \end{pmatrix} \left(1 + c_d \frac{h}{v} + c_{2d} \frac{h^2}{v^2} + \dots \right) + \text{h.c.} \\
& -m_{\ell,i}(\bar{\nu}_{L,i}, \bar{\ell}_{L,i}) \Sigma \begin{pmatrix} 0 \\ \ell_{R,i} \end{pmatrix} \left(1 + c_\ell \frac{h}{v} + c_{2\ell} \frac{h^2}{v^2} + \dots \right) + \text{h.c.}, \quad (3.17)
\end{aligned}$$

where $V(h)$ is the potential of the scalar field

$$V(h) = \frac{m_h^2}{2} h^2 + \frac{d_3}{6} \left(\frac{3m_h^2}{v} \right) h^3 + \frac{d_4}{24} \left(\frac{3m_h^2}{v^2} \right) h^4 + \dots \quad (3.18)$$

The SM corresponds to the choice $a = b = c_u = c_d = c_\ell = d_3 = d_4 = 1$ and $c_{2u} = c_{2d} = c_{2\ell} = 0$. The dominant deviations from the SM in EWPO are induced by

m_t [GeV]	large- m_t expansion	Using ref. [16, 83]
173.2 ± 0.9	1.024 ± 0.021	1.024 ± 0.022
173.3 ± 2.8	1.025 ± 0.030	1.027 ± 0.031

Table 7. Fit result for the HVV coupling a , obtained with different choices for m_t and for the two-loop fermionic EW corrections to ρ_Z^f . When using ref. [16, 83], we do not impose constraints from Γ_Z , σ_h^0 and R_ℓ^0 .

the non-standard coupling $a \neq 1$. This generates extra contributions to the S and T parameters [119]:

$$S = \frac{1}{12\pi}(1 - a^2) \ln \left(\frac{\Lambda^2}{m_h^2} \right), \quad (3.19)$$

$$T = -\frac{3}{16\pi c_W^2}(1 - a^2) \ln \left(\frac{\Lambda^2}{m_h^2} \right), \quad (3.20)$$

where $\Lambda = 4\pi v/\sqrt{|1 - a^2|}$ is the cutoff of the light Higgs effective Lagrangian. A sum rule for $1 - a^2$ can be written in terms of the total cross sections in different isospin channels of longitudinal EW gauge boson scattering [120], implying $a^2 \leq 1$ unless the $I = 2$ channel dominates the cross section. Thus, we expect in general a positive S and a negative T .

We fit the coupling a together with the five SM parameters to the precision observables using the large- m_t expansion for the two-loop fermionic EW corrections to ρ_Z^f , and obtain the results shown in the left plot in figure 7 and reported in table 7. The correlation matrices for the posteriors are given in tables 20 and 21 for the case of m_t from Tevatron pole mass average. In table 7 we also present the result obtained using m_t from the $\overline{\text{MS}}$ mass and including the subleading two-loop fermionic EW corrections to $\delta\rho_Z^f$ with the results of ref. [16, 83]. As is evident from the table, the results are stable against the treatment of $\delta\rho_Z^f$, but the error is sensitive to the uncertainty in m_t . This can be understood by looking at the impact of the individual constraints on a shown in the center plot in figure 7, from which it is evident that M_W is giving the strongest bound on the nonstandard Higgs coupling. Our result is compatible with the analysis of ref. [121].

Since the fit prefers values of $a > 1$, while the sum rule of ref. [120] gives in general $a < 1$, additional contributions to the EWPO, for example from additional light fermions [119, 122], are required in order to restore the agreement with experimental data in composite Higgs models. If one takes literally the model with no new particles below the cutoff and assuming $a \leq 1$, from the 95% probability range $a \in [0.984, 1.070]$ ($[0.981, 1.071]$) one can derive a lower bound on Λ :

$$\Lambda > 17(16) \text{ TeV @95\% probability}, \quad (3.21)$$

using the large- m_t expansion (using the results of ref. [16, 83]). One can generalise the analysis allowing for $\Lambda < 4\pi v/\sqrt{|1 - a^2|}$ and assuming that the dynamics at the cutoff does not contribute sizably to S and T . In this case one can determine regions in the a - Λ plane as shown in right plot of figure 7. Clearly the value of a is tightly constrained for values of Λ compatible with direct searches.

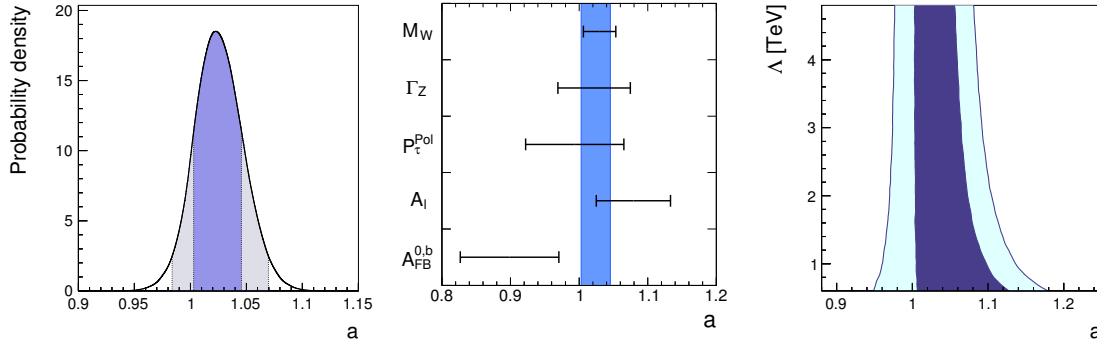


Figure 7. Left: Probability distribution for the coupling a . Center: Indirect determinations of the coupling a , excluding the observables M_W , Γ_Z , P_τ^{pol} , A_l^0 and $A_{\text{FB}}^{0,b}$, except for the one specified in each row. The vertical blue band represents the one obtained from the fit with all the observables. Right: Probability regions in the a - Λ plane. In all plots, the large- m_t expansion is adopted to the two-loop fermionic EW corrections to ρ_Z^f .

3.5 General bounds on the New Physics scale

Before concluding, let us take a more general approach and consider the contributions to the EW fit of arbitrary dimension-six NP-induced operators [11, 20, 123]:

$$\mathcal{L}_{\text{eff}} = \mathcal{L}_{\text{SM}} + \sum_i \frac{C_i}{\Lambda^2} \mathcal{O}_i. \quad (3.22)$$

For concreteness, let us use the same operator basis of ref. [11]:

$$\begin{aligned} \mathcal{O}_{WB} &= (H^\dagger \tau^a H) W_{\mu\nu}^a B^{\mu\nu}, & \mathcal{O}_H &= |H^\dagger D_\mu H|^2, \\ \mathcal{O}_{LL} &= \frac{1}{2} (\bar{L} \gamma_\mu \tau^a L)^2, & \mathcal{O}'_{HL} &= i (H^\dagger D_\mu \tau^a H) (\bar{L} \gamma^\mu \tau^a L), \\ \mathcal{O}'_{HQ} &= i (H^\dagger D_\mu \tau^a H) (\bar{Q} \gamma^\mu \tau^a Q), & \mathcal{O}_{HL} &= i (H^\dagger D_\mu H) (\bar{L} \gamma^\mu L), \\ \mathcal{O}_{HQ} &= i (H^\dagger D_\mu H) (\bar{Q} \gamma^\mu Q), & \mathcal{O}_{HE} &= i (H^\dagger D_\mu H) (\bar{E} \gamma^\mu E), \\ \mathcal{O}_{HU} &= i (H^\dagger D_\mu H) (\bar{U} \gamma^\mu U), & \mathcal{O}_{HD} &= i (H^\dagger D_\mu H) (\bar{D} \gamma^\mu D), \end{aligned} \quad (3.23)$$

where we add the contribution of the Hermitian conjugate for operators \mathcal{O}'_{HL} to \mathcal{O}_{HD} . The Higgs field gets a vev $\langle H \rangle = (0, v/\sqrt{2})^T$. For fermions, we do not consider generation mixing, and assume lepton-flavour universality: $C'_{HL} = C'_{HL_i}$, $C_{HL} = C_{HL_i}$ and $C_{HE} = C_{HE_i}$ for $i = 1, 2, 3$.

The first two operators contribute to the oblique parameters S and T :

$$S = \frac{4s_W c_W C_{WB}}{\alpha(M_Z^2)} \left(\frac{v}{\Lambda}\right)^2, \quad (3.24)$$

$$T = -\frac{C_H}{2\alpha(M_Z^2)} \left(\frac{v}{\Lambda}\right)^2, \quad (3.25)$$

where \mathcal{O}_H violates the custodial symmetry, since it gives a correction to the mass of the Z boson, but not to that of the W boson. The next two operators yield non-oblique

Coefficient	Large- m_t expansion			Using ref. [16, 83]		
	C_i/Λ^2 [TeV $^{-2}$]	Λ [TeV]		C_i/Λ^2 [TeV $^{-2}$]	Λ [TeV]	
	at 95%	$C_i = -1$	$C_i = 1$	at 95%	$C_i = -1$	$C_i = 1$
C_{WB}	[−0.0096, 0.0042]	10.2	15.4	[−0.0095, 0.0045]	10.3	15.0
C_H	[−0.030, 0.007]	5.8	12.1	[−0.031, 0.008]	5.7	11.5
C_{LL}	[−0.011, 0.019]	9.5	7.2	[−0.016, 0.023]	8.0	6.6
C'_{HL}	[−0.012, 0.005]	9.2	14.1	[−0.017, 0.009]	7.6	10.8
C'_{HQ}	[−0.010, 0.015]	10.2	8.2	[−0.40, 0.20]	1.6	2.2
C_{HL}	[−0.007, 0.010]	12.2	10.0	[−0.034, 0.022]	5.5	6.7
C_{HQ}	[−0.023, 0.046]	6.6	4.7	[−0.01, 0.11]	11.7	3.0
C_{HE}	[−0.014, 0.008]	8.4	11.1	[−0.029, 0.019]	5.9	7.2
C_{HU}	[−0.061, 0.087]	4.0	3.4	[−0.37, 0.08]	1.6	3.5
C_{HD}	[−0.15, 0.05]	2.6	4.6	[−1.1, −0.2]	1.0	—

Table 8. Fit results for the coefficients of the dimension six operators at 95% probability in units of $1/\Lambda^2$ TeV $^{-2}$, with quark-flavour universality in NP contribution. The fit is performed switching on one operator at a time. The corresponding lower bounds on the NP scale in TeV obtained by setting $C_i = \pm 1$ are also presented. When using the results from ref. [16, 83], we do not consider constraints from Γ_Z , σ_h^0 and R_t^0 .

corrections to the Fermi constant:

$$G_\mu = G_{\mu,\text{SM}} \left[1 - C_{LL} \left(\frac{v}{\Lambda} \right)^2 + 2 C'_{HL} \left(\frac{v}{\Lambda} \right)^2 \right], \quad (3.26)$$

where $G_{\mu,\text{SM}}$ denotes the Fermi constant in the SM. The corrections to the Fermi constant affect the mass and width of the W boson and the $Zf\bar{f}$ couplings as shown in Appendix A.

The width of the W boson also receives the corrections from the operators \mathcal{O}'_{HL} and \mathcal{O}'_{HQ} :

$$\Gamma_W = \Gamma_{W,\text{SM}} \left[1 + (3C'_{HL} + C'_{HQ_1} + C'_{HQ_2}) \left(\frac{v}{\Lambda} \right)^2 \right]. \quad (3.27)$$

Finally, the operators from \mathcal{O}'_{HL} to \mathcal{O}_{HD} contribute to the $Zf\bar{f}$ couplings:

$$\begin{aligned} \delta g_L^{v_i} &= \frac{C'_{HL_i} - C_{HL_i}}{2} \left(\frac{v}{\Lambda} \right)^2, & \delta g_L^{e_i} &= -\frac{C'_{HL_i} + C_{HL_i}}{2} \left(\frac{v}{\Lambda} \right)^2, \\ \delta g_L^{u_i} &= \frac{C'_{HQ_i} - C_{HQ_i}}{2} \left(\frac{v}{\Lambda} \right)^2, & \delta g_L^{d_i} &= -\frac{C'_{HQ_i} + C_{HQ_i}}{2} \left(\frac{v}{\Lambda} \right)^2, \\ \delta g_R^{e_i} &= -\frac{C_{HE_i}}{2} \left(\frac{v}{\Lambda} \right)^2, & \delta g_R^{u_i} &= -\frac{C_{HU_i}}{2} \left(\frac{v}{\Lambda} \right)^2, & \delta g_R^{d_i} &= -\frac{C_{HD_i}}{2} \left(\frac{v}{\Lambda} \right)^2, \end{aligned} \quad (3.28)$$

where the shifts in the vector and axial-vector couplings are given by $\delta g_V^f = \delta g_L^f + \delta g_R^f$ and $\delta g_A^f = \delta g_L^f - \delta g_R^f$, respectively.

Switching on one operator at a time (thus barring accidental cancellations), one can constrain the coefficient of each of the above operators using the EW fit. Clearly, as is the case for all indirect constraints, one can either interpret this as a bound on the NP scale

Coefficient	Large- m_t expansion			Using ref. [16, 83]		
	C_i/Λ^2 [TeV $^{-2}$]	Λ [TeV]		C_i/Λ^2 [TeV $^{-2}$]	Λ [TeV]	
	at 95%	$C_i = -1$	$C_i = 1$	at 95%	$C_i = -1$	$C_i = 1$
C'_{HQ_1}	[-0.026, 0.034]	6.2	5.4	[-0.19, 0.01]	2.3	11.9
C'_{HQ_2}	[-0.026, 0.034]	6.2	5.4	[-0.20, 0.01]	2.3	10.8
C'_{HQ_3}, C_{HQ_3}	[-0.025, 0.053]	6.3	4.3	[0.00, 0.10]	15.6	3.1
C_{HQ_1}	[-0.26, 0.34]	2.0	1.7	[-1.9, 0.1]	0.7	3.9
C_{HQ_2}	[-0.16, 0.18]	2.5	2.4	[-0.25, 0.15]	2.0	2.6
C_{HU_1}	[-0.13, 0.17]	2.8	2.4	[-0.97, 0.03]	1.0	5.6
C_{HU_2}	[-0.11, 0.17]	3.0	2.4	[-0.39, 0.21]	1.6	2.2
C_{HD_1}, C_{HD_2}	[-0.34, 0.26]	1.7	2.0	[-0.1, 1.9]	3.8	0.7
C_{HD_3}	[-0.38, 0.03]	1.6	6.3	[-0.66, -0.13]	1.2	—

Table 9. Same as table 8, but without quark-flavour universality. The operator \mathcal{O}_{HU_3} does not contribute to the EWPO.

fixing the coupling or as a bound on the coupling for fixed NP scale. In tables 8 and 9, we list for all the operators the 95% probability regions of the coefficients and the lower bound on the NP scale in TeV obtained by setting $C_i = \pm 1$, with and without quark-flavour universality for the operators. Comparing these results with the ones of ref. [11], we see that the recent experimental improvements strengthen the bounds on NP contributions, pushing the lower bound on Λ to scales as large as 15 TeV.

Moreover, we also fit multiple coefficients simultaneously by dividing the operators into three categories: the oblique operators \mathcal{O}_{WB} and \mathcal{O}_H , the four-fermion operator \mathcal{O}_{LL} , and the operators with scalars and fermions. Since one cannot determine all the operators simultaneously from the EWPO alone, we fit a part of them turning on the operators in each category. The fit results are summarized in table 10, with and without assuming quark-flavour universality (the results for \mathcal{O}_{LL} can be found in table 8). When we use the results of ref. [16, 83] dropping Γ_Z , σ_h^0 and R_ℓ^0 from the fit, we cannot determine individually the coefficients C_{HL} and C_{HE} , but only the combination

$$C[\mathcal{A}_\ell] = \left(g_L^\ell \delta g_R^\ell - g_R^\ell \delta g_L^\ell \right) \left(\frac{\Lambda}{v} \right)^2, \quad (3.29)$$

which is associated with \mathcal{A}_ℓ , can be constrained. For the fit without universality, we float the coefficients C'_{HL} , C'_{HQ_i} , C_{HL} , C_{HQ_i} , C_{HE} , C_{HU_i} , C_{HD_i} for $i = 1, 2$ and 3, except for C_{HU_3} , together with the SM parameters, and obtain the posteriors listed in table 10. The combinations $C'_{HQ_1} + C'_{HQ_2}$, $C'_{HQ_2} - C_{HQ_2}$, $C'_{HQ_3} + C_{HQ_3}$ and $C[\Gamma_{uds}]$, are associated with Γ_W , g_L^c , g_L^b and the light-quark contribution to Γ_Z respectively, where the last combination is defined as

$$C[\Gamma_{uds}] = \sum_{f=u,d,s} \left(g_L^f \delta g_L^f + g_R^f \delta g_R^f \right) \left(\frac{\Lambda}{v} \right)^2. \quad (3.30)$$

The correlations of the fit results are summarized in tables 22-27.

	Large- m_t expansion	Using ref. [16, 83]
Coefficient	C_i/Λ^2 [TeV $^{-2}$] at 95%	C_i/Λ^2 [TeV $^{-2}$] at 95%
C_{WB}	[−0.009, 0.018]	[−0.009, 0.021]
C_H	[−0.058, 0.015]	[−0.068, 0.016]
C'_{HL}	[−0.026, 0.008]	[−0.029, 0.006]
C'_{HQ}	[−0.18, 0.00]	[−0.34, 0.31]
C_{HL}	[−0.013, 0.020]	—
C_{HQ}	[−0.11, 0.07]	[−0.07, 0.12]
C_{HE}	[−0.022, 0.018]	—
C_{HU}	[−0.22, 0.41]	[−0.26, 0.49]
C_{HD}	[−1.2, −0.2]	[−1.2, −0.2]
$C[\mathcal{A}_\ell]$	—	[−0.0021, 0.0050]
C'_{HL}	[−0.026, 0.008]	[−0.029, 0.006]
C_{HL}	[−0.013, 0.020]	—
C_{HE}	[−0.022, 0.018]	—
C_{HU_2}	[−0.22, 0.45]	[−0.32, 0.55]
C_{HD_3}	[−1.2, −0.2]	[−1.2, −0.2]
$C'_{HQ_1} + C'_{HQ_2}$	[−0.59, 0.51]	[−0.68, 0.61]
$C'_{HQ_2} - C_{HQ_2}$	[−0.30, 0.17]	[−0.67, 0.55]
$C'_{HQ_3} + C_{HQ_3}$	[−0.22, −0.01]	[−0.77, 0.63]
$C[\mathcal{A}_\ell]$	—	[−0.0021, 0.0050]
$C[\Gamma_{uds}]$	[−0.039, 0.044]	[−0.42, 0.43]

Table 10. Fit results for the coefficients of the dimension six operators at 95% probability in units of $1/\Lambda^2$ TeV $^{-2}$. We perform three separate fits, for the oblique operators \mathcal{O}_{WB} and \mathcal{O}_H , for the non-oblique operators, except for \mathcal{O}_{LL} , with quark-flavour universality, and for the non-oblique operators, except for \mathcal{O}_{LL} , without quark-flavour universality. When we use the results of ref. [16, 83], we cannot determine individually the coefficients C_{HL} and C_{HE} but only the combination $C[\mathcal{A}_\ell]$, since the observables Γ_Z , σ_h^0 and R_ℓ^0 have been neglected.

A similar analysis was recently performed in ref. [20]. The constraints on C_{WB}/Λ^2 and C_H/Λ^2 correspond to those on $\tan\theta_W(\bar{c}_W + \bar{c}_B)/v^2$ and $-2\bar{c}_T/v^2$ in ref. [20], respectively, while the other coefficients satisfy the relations $C_i/\Lambda^2 = \bar{c}_i/v^2$. Our results in table 10 are generally similar to theirs, although one cannot directly compare the results since we have floated a larger set of operators simultaneously. Our fit results are also compatible with the ones of ref. [124], considering that in the latter work m_h was not yet available and that in the fit the other SM parameters were not floated.

All the results presented here refer to coefficients computed at the weak scale. While other choices of operator basis could be more convenient to study running effects (see refs. [125–127]) or additional observables such as in ref. [20], for our purpose the basis of ref. [11] is perfectly adequate.

4 Summary

With the recent discovery of the Higgs boson and the persistent absence of any direct signal of NP, indirect searches represent even more than before the best strategy to probe physics beyond the SM. In particular, EWPO offer a very powerful handle on the mechanism of EWSB and allow us to strongly constrain any NP relevant to solve the hierarchy problem. In this context, we have presented an updated fit of EWPO in the SM and beyond, obtained using a new code tested against the ZFITTER one. We have discussed in detail the impact of the recently computed two-loop fermionic EW corrections to the $Zf\bar{f}$ vertices, stressing the need for an independent evaluation of these corrections for individual fermions. Our results in the SM are summarized in tables 1, 2 and 3. We have obtained bounds on oblique NP contributions (see table 4) and on ϵ parameters (see table 5), as well as SM predictions for ϵ_i in eq. (3.15). We have derived constraints on modified $Zb\bar{b}$ couplings, see table 6. We have studied the bounds from EWPO on the Higgs coupling to vector bosons, obtaining the results in table 7, hinting at an elementary Higgs boson or at a nontrivial composite Higgs model. Finally, we have updated the constraints on the NP-induced dimension-six operators relevant for the EWPO, reported in tables 8, 9 and 10.

A graphical summary of the result for each observable is presented in Appendices D and E.

While the results we obtained are consistent with the non-observation of NP at the 7 and 8-TeV runs, the possibility of weakly-interacting NP hiding behind the corner remains unscathed.

Acknowledgments

M.C. is associated to the Dipartimento di Matematica e Fisica, Università di Roma Tre, and E.F. and L.S. are associated to the Dipartimento di Fisica, Università di Roma “La Sapienza”. We are indebted to R. Contino for stimulating discussions and suggestions, and for his careful comparison of our preliminary results with the literature. We are grateful to A. Freitas for providing us with details of his computations and unpublished results. We thank J. de Blas, G. Degrassi, G. Grilli di Cortona and A. Strumia for useful discussions and comments. We acknowledge useful discussions with T. Riemann on the comparison of our results with the ZFITTER ones. We thank the BAT authors, in particular F. Beaujean and D. Kollar, for precious support on the usage of their toolkit. M.C, E.F and L.S. acknowledge partial support from MIUR (Italy) under the PRIN 2010-2011 program. The research leading to these results has received funding from the European Research Council under the European Union’s Seventh Framework Programme (FP/2007-2013) / ERC Grant Agreements n. 279972 and n. 267985.

A NP contributions to the EW precision observables

We express each observable as a linear function of the NP parameters as in refs. [4, 99–102]. Here we use s_W^2 , c_W^2 , g_V^f and g_A^f for the corresponding SM values, and write the shift to

the Fermi constant as $G_\mu = G_{\mu,\text{SM}}(1 + \Delta G)$. The corrections to the mass and width⁸ of the W boson are then given by

$$M_W = M_{W,\text{SM}} \left[1 - \frac{\alpha(M_Z^2)}{4(c_W^2 - s_W^2)} \left(S - 2c_W^2 T - \frac{c_W^2 - s_W^2}{2s_W^2} U \right) - \frac{s_W^2}{2(c_W^2 - s_W^2)} \Delta G \right], \quad (\text{A.1})$$

$$\Gamma_W = \Gamma_{W,\text{SM}} \left[1 - \frac{3\alpha(M_Z^2)}{4(c_W^2 - s_W^2)} \left(S - 2c_W^2 T - \frac{c_W^2 - s_W^2}{2s_W^2} U \right) - \frac{1 + c_W^2}{2(c_W^2 - s_W^2)} \Delta G \right], \quad (\text{A.2})$$

where $\Gamma_{W,\text{SM}}$ is given in terms of G_μ , $M_{W,\text{SM}}$ and so forth. Moreover, the shifts in the $Zf\bar{f}$ couplings read

$$\delta g_V^f = \frac{g_V^f}{2} [\alpha(M_Z^2) T - \Delta G] + \frac{(g_V^f - g_A^f) [\alpha(M_Z^2) (S - 4c_W^2 s_W^2 T) + 4c_W^2 s_W^2 \Delta G]}{4s_W^2 (c_W^2 - s_W^2)}, \quad (\text{A.3})$$

$$\delta g_A^f = \frac{g_A^f}{2} [\alpha(M_Z^2) T - \Delta G], \quad (\text{A.4})$$

where we neglect the imaginary parts of the SM couplings in NP contributions below. Using these couplings and defining the following quantities

$$G_f \equiv (g_V^f)^2 + (g_A^f)^2, \quad \delta G_f \equiv 2(g_V^f \delta g_V^f + g_A^f \delta g_A^f), \quad (\text{A.5})$$

the Z -pole observables are written as

$$\sin^2 \theta_{\text{eff}}^{\text{lept}} = \sin^2 \theta_{\text{eff,SM}}^{\text{lept}} - \frac{g_A^e \delta g_V^e - g_V^e \delta g_A^e}{4(g_A^e)^2}, \quad (\text{A.6})$$

$$\mathcal{A}_f = \mathcal{A}_{f,\text{SM}} - \frac{2[(g_V^f)^2 - (g_A^f)^2]}{G_f^2} (g_A^f \delta g_V^f - g_V^f \delta g_A^f), \quad (\text{A.7})$$

$$A_{\text{FB}}^{0,f} = A_{\text{FB,SM}}^{0,f} - \left[\frac{3g_V^f g_A^f [(g_V^e)^2 - (g_A^e)^2]}{G_f G_e^2} (g_A^e \delta g_V^e - g_V^e \delta g_A^e) + (e \leftrightarrow f) \right], \quad (\text{A.8})$$

$$\Gamma_Z = \Gamma_{Z,\text{SM}} + \frac{\alpha(M_Z^2) M_Z}{12s_W^2 c_W^2} \sum_f N_c^f \delta G_f, \quad (\text{A.9})$$

$$\sigma_h^0 = \sigma_{h,\text{SM}}^0 + \frac{12\pi G_e (\sum_q N_c^q G_q)}{M_Z^2 (\sum_f N_c^f G_f)^2} \left(\frac{\delta G_e}{G_e} + \frac{\sum_q \delta G_q}{\sum_q G_q} - \frac{2 \sum_f N_c^f \delta G_f}{\sum_f N_c^f G_f} \right), \quad (\text{A.10})$$

$$R_\ell^0 = R_{\ell,\text{SM}}^0 + \frac{\sum_q N_c^q \delta G_q}{G_\ell} - \frac{(\sum_q N_c^q G_q) \delta G_\ell}{G_\ell^2}, \quad (\text{A.11})$$

$$R_c^0 = R_{c,\text{SM}}^0 + \frac{\delta G_c}{\sum_q G_q} - \frac{G_c \sum_q \delta G_q}{(\sum_q G_q)^2}, \quad (\text{A.12})$$

$$R_b^0 = R_{b,\text{SM}}^0 + \frac{\delta G_b}{\sum_q G_q} - \frac{G_b \sum_q \delta G_q}{(\sum_q G_q)^2}, \quad (\text{A.13})$$

where $N_c^f = 3$ for quarks and $N_c^f = 1$ for leptons.

⁸Our formula for the W -boson width in eq. (A.2) differs from that in ref. [100, 101], since we have expressed the W -boson mass appearing in the phase-space factor in terms of the NP parameters.

B Non-universal vertex corrections

As shown in eqs. (3.6)-(3.11), the parameters ϵ_1 , ϵ_2 and ϵ_3 are defined from the $Ze\bar{e}$ effective couplings. To apply the same parameters to other decay channels, flavour non-universal vertex corrections have to be taken into account. Below we summarize the formulæ of the non-universal corrections at one-loop level, which can be found in ref. [79] and references therein.

The non-universal corrections to the effective couplings ρ_Z^f and κ_Z^f are given by

$$\begin{aligned}\Delta\rho_Z^f &= \rho_Z^f - \rho_Z^e = \frac{\alpha}{2\pi s_W^2} (u_f - u_e), \\ \Delta\kappa_Z^f &= \kappa_Z^f - \kappa_Z^e = \frac{\alpha}{4\pi s_W^2} \left(\frac{\delta_f^2 - \delta_e^2}{4c_W^2} \mathcal{F}_Z(M_Z^2) - u_f + u_e \right),\end{aligned}\quad (\text{B.1})$$

respectively, where u_f and δ_f are defined as

$$\begin{aligned}u_f &= \frac{3v_f^2 + a_f^2}{4c_W^2} \mathcal{F}_Z(M_Z^2) + \mathcal{F}_W^f(M_Z^2), \\ \delta_f &= v_f - a_f\end{aligned}\quad (\text{B.2})$$

with the tree-level vector and axial-vector couplings $v_f = I_3^f - 2Q_f s_W^2$ and $a_f = I_3^f$. The so-called unified form factors \mathcal{F}_Z and \mathcal{F}_W^f , associated with the radiative corrections to the $Zf\bar{f}$ vertices with a virtual Z boson and with a virtual W boson(s), respectively, are given as follows:

$$\begin{aligned}\mathcal{F}_Z(s) &= \mathcal{F}_{Za}(s), \\ \mathcal{F}_W^f(s) &= c_W^2 \mathcal{F}_{Wn}(s) - \frac{1}{2} |\sigma_{f'}| \mathcal{F}_{Wa}(s) - \frac{1}{2} \bar{\mathcal{F}}_{Wa}(s),\end{aligned}\quad (\text{B.3})$$

where $|\sigma_{f'}| = |v_{f'} + a_{f'}|$ with f' being the partner of f in the $SU(2)_L$ doublet, and the subscripts “ a ” and “ n ” stand for contributions from abelian and non-abelian diagrams, respectively. In the limit of massless fermions, the form factors are written with the loop functions B_0 and C_0 :

$$\begin{aligned}\mathcal{F}_{Va}(s) &= 2(R_V + 1)^2 s C_0(s; 0, (\widetilde{M}_V^2)^{1/2}, 0) - (2R_V + 3) \ln \left(-\frac{\widetilde{M}_V^2}{s} \right) - 2R_V - \frac{7}{2}, \\ \mathcal{F}_{Wn}(s) &= -2(R_W + 2)M_W^2 C_0(s; M_W, 0, M_W) + 2R_W + \frac{9}{2} - \frac{11}{18R_W} + \frac{1}{18R_W^2} \\ &\quad - \left(2R_W + \frac{7}{3} - \frac{3}{2R_W} - \frac{1}{12R_W^2} \right) B_0(\mu; s; M_W, M_W), \\ \bar{\mathcal{F}}_{Wa}(s) &= 0,\end{aligned}\quad (\text{B.4})$$

where $\widetilde{M}_V^2 \equiv M_V^2 - iM_V\Gamma_V \approx M_V^2 - i\varepsilon$, and $R_V = M_V^2/s$ for $V = Z, W$. The scalar two-point function B_0 and the scalar three-point function C_0 are defined by

$$B_0(\mu; p^2; m_0, m_1) = \frac{(2\pi\mu)^{4-d}}{i\pi^2} \int d^d k \frac{1}{(k^2 - m_0^2 + i\varepsilon) [(k+p)^2 - m_1^2 + i\varepsilon]}, \quad (\text{B.5})$$

$$C_0(p^2; m_0, m_1, m_0) = -\frac{1}{i\pi^2} \int d^4k \frac{1}{(k^2 - m_1^2 + i\varepsilon) [(k + p_1)^2 - m_0^2 + i\varepsilon] [(k - p_2)^2 - m_0^2 + i\varepsilon]}, \quad (\text{B.6})$$

where μ is the renormalization scale in the former, and $p_1^2 = p_2^2 = 0$ and $p^2 = (p_1 + p_2)^2$ in the latter. Note that the contributions from $\mathcal{F}_{Wn}(s)$ cancel out in eq. (B.1).

In the case of $f = b$, the additional non-universal corrections associated with the heavy top-quark loop are parameterized by ϵ_b as shown in eq. (3.14).

C Correlation matrices for fit results

	α_s	$\Delta\alpha_{\text{had}}^{(5)}$	M_Z	m_t	m_h	$\delta\rho_Z^\nu$	$\delta\rho_Z^\ell$	$\delta\rho_Z^b$
α_s	1.00							
$\Delta\alpha_{\text{had}}^{(5)}$	-0.01	1.00						
M_Z	0.00	0.08	1.00					
m_t	0.01	0.18	-0.05	1.00				
m_h	0.00	-0.01	0.00	0.00	1.00			
$\delta\rho_Z^\nu$	0.00	-0.01	-0.05	-0.02	0.00	1.00		
$\delta\rho_Z^\ell$	0.00	0.02	-0.10	-0.08	0.00	0.49	1.00	
$\delta\rho_Z^b$	-0.18	0.10	-0.02	-0.06	0.00	-0.28	0.38	1.00

Table 11. Correlation matrix for the fit in table 1.

	α_s	$\Delta\alpha_{\text{had}}^{(5)}$	M_Z	m_t	m_h
α_s	1.00				
$\Delta\alpha_{\text{had}}^{(5)}$	0.01	1.00			
M_Z	0.00	0.09	1.00		
m_t	0.01	0.19	-0.06	1.00	
m_h	0.00	0.00	0.00	0.00	1.00

Table 12. Correlation matrix for the fit in table 2.

	S	T	U	α_s	$\Delta\alpha_{\text{had}}^{(5)}$	M_Z	m_t	m_h
S	1.00							
T	0.85	1.00						
U	-0.48	-0.79	1.00					
α_s	-0.07	-0.10	0.10	1.00				
$\Delta\alpha_{\text{had}}^{(5)}$	-0.30	0.00	-0.09	0.00	1.00			
M_Z	-0.05	-0.10	0.03	0.01	0.00	1.00		
m_t	0.02	-0.07	-0.04	0.01	0.00	0.00	1.00	
m_h	0.00	0.00	0.00	0.00	0.00	0.00	0.00	1.00

Table 13. Correlation matrix for the fit results in the second column of table 4.

	S	T	α_s	$\Delta\alpha_{\text{had}}^{(5)}$	M_Z	m_t	m_h
S	1.00						
T	0.86	1.00					
α_s	-0.03	-0.03	1.00				
$\Delta\alpha_{\text{had}}^{(5)}$	-0.40	-0.12	0.01	1.00			
M_Z	-0.04	-0.12	0.00	0.00	1.00		
m_t	0.00	-0.17	0.01	0.00	0.00	1.00	
m_h	0.00	0.00	0.00	0.00	0.00	0.00	1.00

Table 14. Correlation matrix for the fit results in the third column of table 4.

	S	T	α_s	$\Delta\alpha_{\text{had}}^{(5)}$	M_Z	m_t	m_h
S	1.00						
T	0.89	1.00					
α_s	0.00	0.01	1.00				
$\Delta\alpha_{\text{had}}^{(5)}$	-0.40	-0.14	0.00	1.00			
M_Z	-0.01	-0.08	0.00	0.00	1.00		
m_t	-0.01	-0.16	0.00	0.00	0.00	1.00	
m_h	0.00	0.00	0.00	0.00	0.00	0.00	1.00

Table 15. Correlation matrix for the fit results in the fourth column of table 4.

	ϵ_1	ϵ_2	ϵ_3	ϵ_b	α_s	$\Delta\alpha_{\text{had}}^{(5)}$	M_Z	m_t	m_h
ϵ_1	1.00								
ϵ_2	0.79	1.00							
ϵ_3	0.86	0.50	1.00						
ϵ_b	-0.32	-0.31	-0.21	1.00					
α_s	-0.06	-0.06	-0.04	-0.12	1.00				
$\Delta\alpha_{\text{had}}^{(5)}$	0.00	0.07	-0.30	0.00	0.00	1.00			
M_Z	-0.10	-0.03	-0.05	0.02	0.00	0.00	1.00		
m_t	0.00	0.00	0.00	0.00	0.00	0.00	0.00	1.00	
m_h	0.00	0.00	0.00	0.00	0.00	0.00	0.00	0.00	1.00

Table 16. Correlation matrix for the fit results in the second column of table 5.

	ϵ_1	ϵ_3	α_s	$\Delta\alpha_{\text{had}}^{(5)}$	M_Z	m_t	m_h
ϵ_1	1.00						
ϵ_3	0.87	1.00					
α_s	-0.04	-0.03	1.00				
$\Delta\alpha_{\text{had}}^{(5)}$	-0.10	-0.39	0.01	1.00			
M_Z	-0.12	-0.04	0.02	0.00	1.00		
m_t	-0.03	-0.01	0.01	-0.01	-0.01	1.00	
m_h	0.00	0.00	0.00	0.00	0.00	0.00	1.00

Table 17. Correlation matrix for the fit results in the third column of table 5.

	δg_R^b	δg_L^b	α_s	$\Delta\alpha_{\text{had}}^{(5)}$	M_Z	m_t	m_h
δg_R^b	1.00						
δg_L^b	0.90	1.00					
α_s	0.04	-0.02	1.00				
$\Delta\alpha_{\text{had}}^{(5)}$	-0.22	-0.21	0.00	1.00			
M_Z	0.01	0.01	0.00	0.08	1.00		
m_t	0.01	0.02	0.00	0.18	-0.06	1.00	
m_h	0.00	0.00	0.00	-0.01	0.00	0.00	1.00

Table 18. Correlation matrix for the fit results in the second column of table 6.

	δg_R^b	δg_L^b	α_s	$\Delta\alpha_{\text{had}}^{(5)}$	M_Z	m_t	m_h
δg_R^b	1.00						
δg_L^b	0.82	1.00					
α_s	-0.01	0.00	1.00				
$\Delta\alpha_{\text{had}}^{(5)}$	-0.19	-0.22	-0.01	1.00			
M_Z	0.01	0.01	0.00	0.08	1.00		
m_t	-0.01	0.02	0.01	0.17	-0.05	1.00	
m_h	0.00	0.00	0.00	0.00	0.00	0.00	1.00

Table 19. Correlation matrix for the fit results in the third column of table 6.

	a	α_s	$\Delta\alpha_{\text{had}}^{(5)}$	M_Z	m_t	m_h
a	1.00					
α_s	-0.02	1.00				
$\Delta\alpha_{\text{had}}^{(5)}$	0.53	0.00	1.00			
M_Z	-0.17	0.00	-0.02	1.00		
m_t	-0.32	0.01	-0.02	0.00	1.00	
m_h	0.01	0.00	0.00	0.00	0.00	1.00

Table 20. Correlation matrix for the fit result in top left entry of table 7.

	a	α_s	$\Delta\alpha_{\text{had}}^{(5)}$	M_Z	m_t	m_h
a	1.00					
α_s	0.02	1.00				
$\Delta\alpha_{\text{had}}^{(5)}$	0.53	0.00	1.00			
M_Z	-0.15	0.00	-0.01	1.00		
m_t	-0.32	0.00	-0.02	0.00	1.00	
m_h	0.01	0.00	0.00	0.00	0.00	1.00

Table 21. Same as table 20 but for the top-right entry.

	C_{WB}	C_H	α_s	$\Delta\alpha_{\text{had}}^{(5)}$	M_Z	m_t	m_h
C_{WB}	1.00						
C_H	-0.86	1.00					
α_s	-0.03	0.03	1.00				
$\Delta\alpha_{\text{had}}^{(5)}$	-0.40	0.12	0.01	1.00			
M_Z	-0.04	0.12	0.00	0.00	1.00		
m_t	0.00	0.17	0.01	0.00	0.00	1.00	
m_h	0.00	0.00	0.00	0.00	0.00	0.00	1.00

Table 22. Correlation matrix for the fit results in table 10 (first set of operators, using the large- m_t expansion).

	C'_{HL}	C'_{HQ}	C_{HL}	C_{HQ}	C_{HE}	C_{HU}	C_{HD}	α_s	$\Delta\alpha_{\text{had}}^{(5)}$	M_Z	m_t	m_h
C'_{HL}	1.00											
C'_{HQ}	0.24	1.00										
C_{HL}	0.56	0.04	1.00									
C_{HQ}	0.00	-0.38	-0.09	1.00								
C_{HE}	0.58	-0.05	0.72	-0.11	1.00							
C_{HU}	-0.01	-0.78	0.05	0.62	0.04	1.00						
C_{HD}	0.01	0.61	-0.24	0.36	-0.26	-0.11	1.00					
α_s	-0.02	-0.03	-0.01	0.00	-0.01	0.00	0.00	1.00				
$\Delta\alpha_{\text{had}}^{(5)}$	-0.36	-0.04	0.12	-0.01	0.12	-0.01	0.01	0.00	1.00			
M_Z	0.16	0.02	0.06	0.00	0.12	0.00	-0.01	0.00	0.00	1.00		
m_t	0.32	0.06	0.12	0.02	0.17	0.00	0.00	0.00	0.00	0.00	1.00	
m_h	-0.01	0.00	0.00	0.00	0.00	0.00	0.00	0.00	0.00	0.00	0.00	1.00

Table 23. Same as table 22, but for the second set of operators.

	C'_{HL}	C_{HL}	C_{HE}	C_{HU_2}	C_{HD_3}	C_{12}	C_2	C_3	$C[\Gamma_{uds}]$	α_s	$\Delta\alpha_{\text{had}}^{(5)}$	M_Z	m_t	m_h
C'_{HL}	1.00													
C_{HL}	0.56	1.00												
C_{HE}	0.58	0.72	1.00											
C_{HU_2}	-0.03	0.04	0.04	1.00										
C_{HD_3}	0.03	-0.23	-0.26	-0.13	1.00									
C_{12}	0.02	0.02	0.01	-0.02	0.00	1.00								
C_2	0.11	0.05	0.02	-0.30	0.14	0.02	1.00							
C_3	0.23	-0.04	-0.14	-0.17	0.87	0.01	0.11	1.00						
$C[\Gamma_{uds}]$	-0.01	0.08	-0.03	-0.30	-0.03	0.00	-0.75	-0.01	1.00					
α_s	-0.02	-0.01	-0.01	0.00	0.00	-0.01	-0.01	-0.03	-0.03	1.00				
$\Delta\alpha_{\text{had}}^{(5)}$	-0.36	0.12	0.12	-0.01	0.00	0.00	-0.02	-0.05	0.04	0.00	1.00			
M_Z	0.16	0.06	0.12	0.00	-0.01	0.00	0.01	0.02	-0.02	0.00	0.00	1.00		
m_t	0.31	0.11	0.16	-0.01	0.01	0.00	0.03	0.08	-0.02	0.00	0.00	0.00	1.00	
m_h	-0.01	0.00	0.00	0.00	0.00	0.00	0.00	0.00	0.00	0.00	0.00	0.00	0.00	1.00

Table 24. Same as table 22, but for the third set of operators, where C_{12} , C_2 and C_3 denote $C'_{HQ_1} + C'_{HQ_2}$, $C'_{HQ_2} - C_{HQ_2}$ and $C'_{HQ_3} + C_{HQ_3}$, respectively.

	C_{WB}	C_H	α_s	$\Delta\alpha_{\text{had}}^{(5)}$	M_Z	m_t	m_h
C_{WB}	1.00						
C_H	-0.89	1.00					
α_s	0.00	-0.01	1.00				
$\Delta\alpha_{\text{had}}^{(5)}$	-0.40	0.15	0.00	1.00			
M_Z	-0.02	0.09	0.00	0.00	1.00		
m_t	-0.02	0.16	0.00	0.00	0.00	1.00	
m_h	0.00	0.00	0.00	0.00	0.00	0.00	1.00

Table 25. Same as table 22, using the results from ref. [16, 83].

	C'_{HL}	C'_{HQ}	C_{HQ}	C_{HU}	C_{HD}	$C[\mathcal{A}_\ell]$	α_s	$\Delta\alpha_{\text{had}}^{(5)}$	M_Z	m_t	m_h
C'_{HL}	1.00										
C'_{HQ}	0.00	1.00									
C_{HQ}	-0.03	0.31	1.00								
C_{HU}	-0.04	0.35	0.70	1.00							
C_{HD}	0.02	-0.12	0.18	-0.25	1.00						
$C[\mathcal{A}_\ell]$	-0.23	0.00	-0.09	0.10	-0.36	1.00					
α_s	-0.02	-0.01	0.01	0.00	0.00	0.01	1.00				
$\Delta\alpha_{\text{had}}^{(5)}$	-0.35	0.01	0.00	0.00	0.00	0.52	0.00	1.00			
M_Z	0.15	0.00	-0.01	0.00	0.00	-0.05	0.00	0.00	1.00		
m_t	0.31	-0.01	0.02	-0.02	0.00	-0.13	0.00	0.00	0.00	1.00	
m_h	-0.01	0.00	0.00	0.00	0.00	0.01	0.00	0.00	0.00	0.00	1.00

Table 26. Same as table 25, but for the second set of operators.

	C'_{HL}	C_{HU_2}	C_{HD_3}	C_{12}	C_2	C_3	$C[\mathcal{A}_\ell]$	$C[\Gamma_{uds}]$	α_s	$\Delta\alpha_{\text{had}}^{(5)}$	M_Z	m_t	m_h
C'_{HL}	1.00												
C_{HU_2}	-0.04	1.00											
C_{HD_3}	0.02	-0.26	1.00										
C_{12}	0.00	0.28	-0.11	1.00									
C_2	0.01	0.50	-0.19	0.43	1.00								
C_3	0.00	0.61	-0.14	0.46	0.92	1.00							
$C[\mathcal{A}_\ell]$	-0.23	0.07	-0.35	0.00	-0.01	-0.04	1.00						
$C[\Gamma_{uds}]$	-0.03	0.61	-0.26	0.46	0.89	0.99	0.01	1.00					
α_s	-0.02	0.00	0.00	0.00	0.00	0.00	0.01	0.00	1.00				
$\Delta\alpha_{\text{had}}^{(5)}$	-0.35	0.00	0.00	0.01	0.00	0.00	0.52	0.01	0.00	1.00			
M_Z	0.15	0.00	0.00	0.00	0.00	0.00	-0.05	-0.01	0.00	0.00	1.00		
m_t	0.31	-0.01	0.00	-0.01	0.00	0.00	-0.13	-0.01	0.00	0.00	0.00	1.00	
m_h	-0.01	0.00	0.00	0.00	0.00	0.00	0.01	0.00	0.00	0.00	0.00	0.00	1.00

Table 27. Same as table 25, but for the third set of operators, where C_{12} , C_2 and C_3 denote $C'_{HQ_1} + C'_{HQ_2}$, $C'_{HQ_2} - C_{HQ_2}$ and $C'_{HQ_3} + C_{HQ_3}$, respectively.

D Fit results for the observables with the large- m_t expansion for two-loop fermionic EW corrections to ρ_Z^f

In this Appendix we present a graphical summary of the fit results for all observables obtained within the various scenarios considered in this work, obtained using the large- m_t expansion for the two-loop fermionic EW corrections to ρ_Z^f . The labels in the figures refer to the various fits performed with a self-explanatory notation. The blue band corresponds to the direct measurement, also reported with the ‘‘Data’’ label.

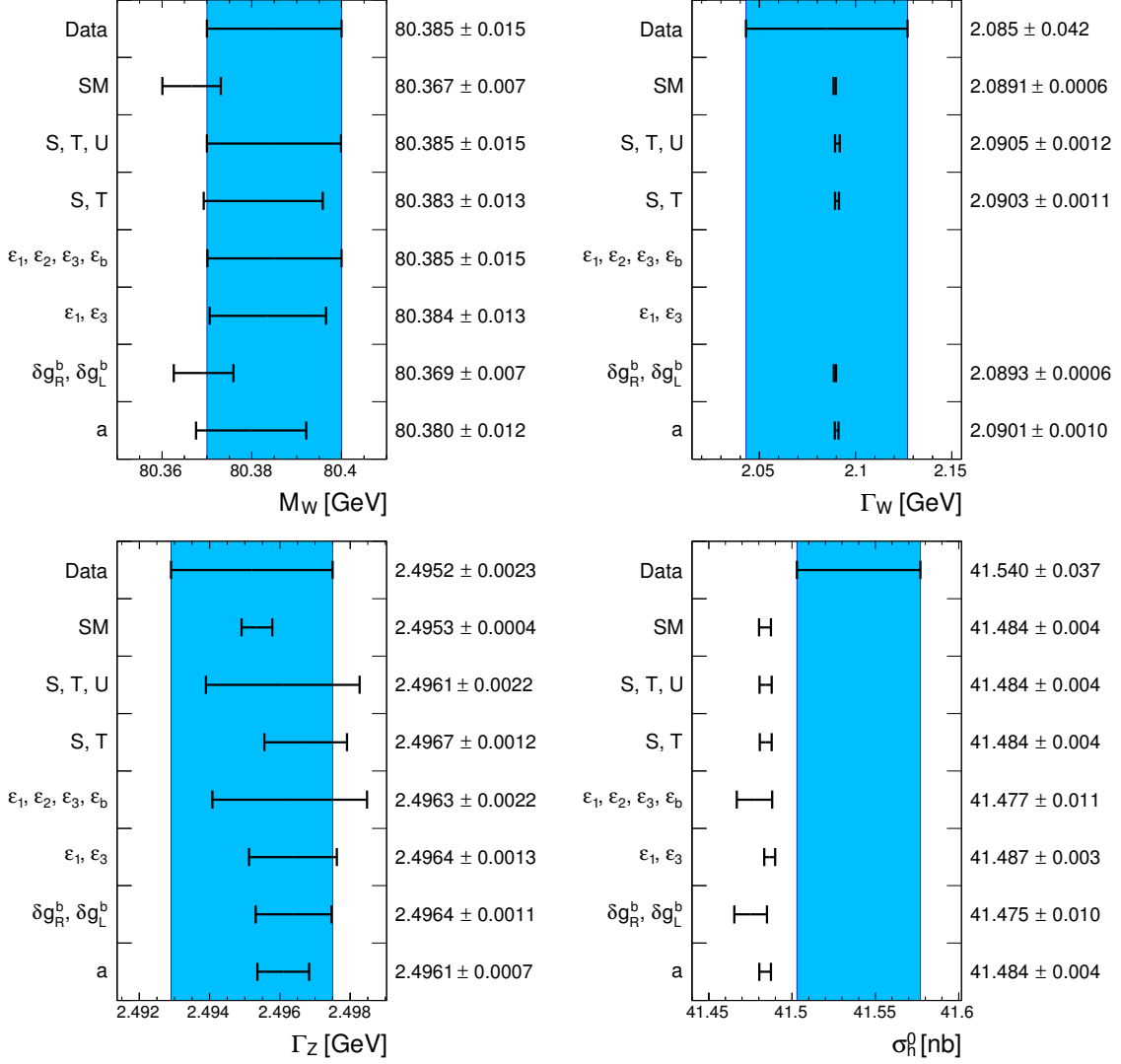


Figure 8. Fit results, with the large- m_t expansion for the two-loop fermionic EW corrections to the coupling ρ_Z^f .

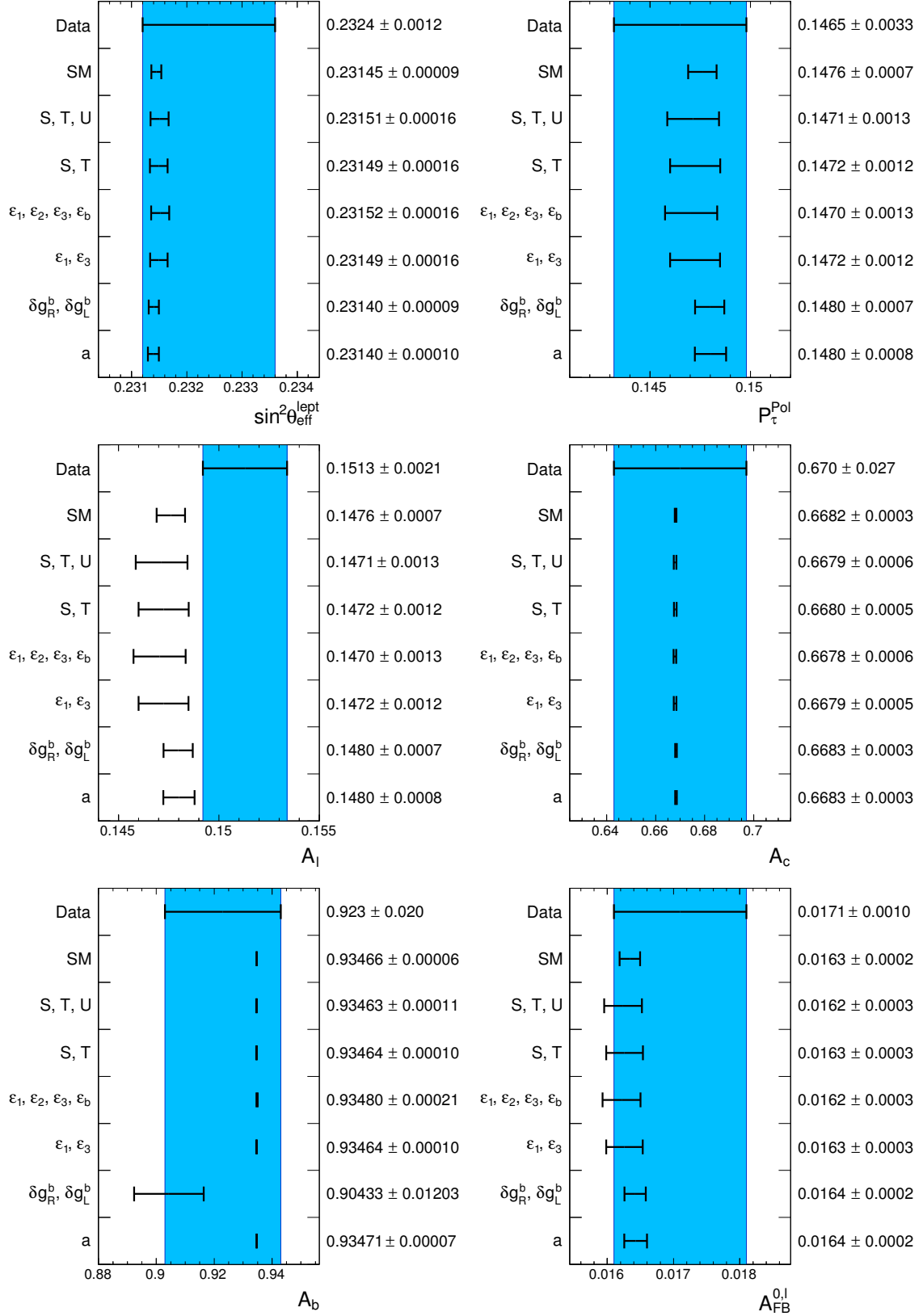


Figure 9. Same as figure 8.

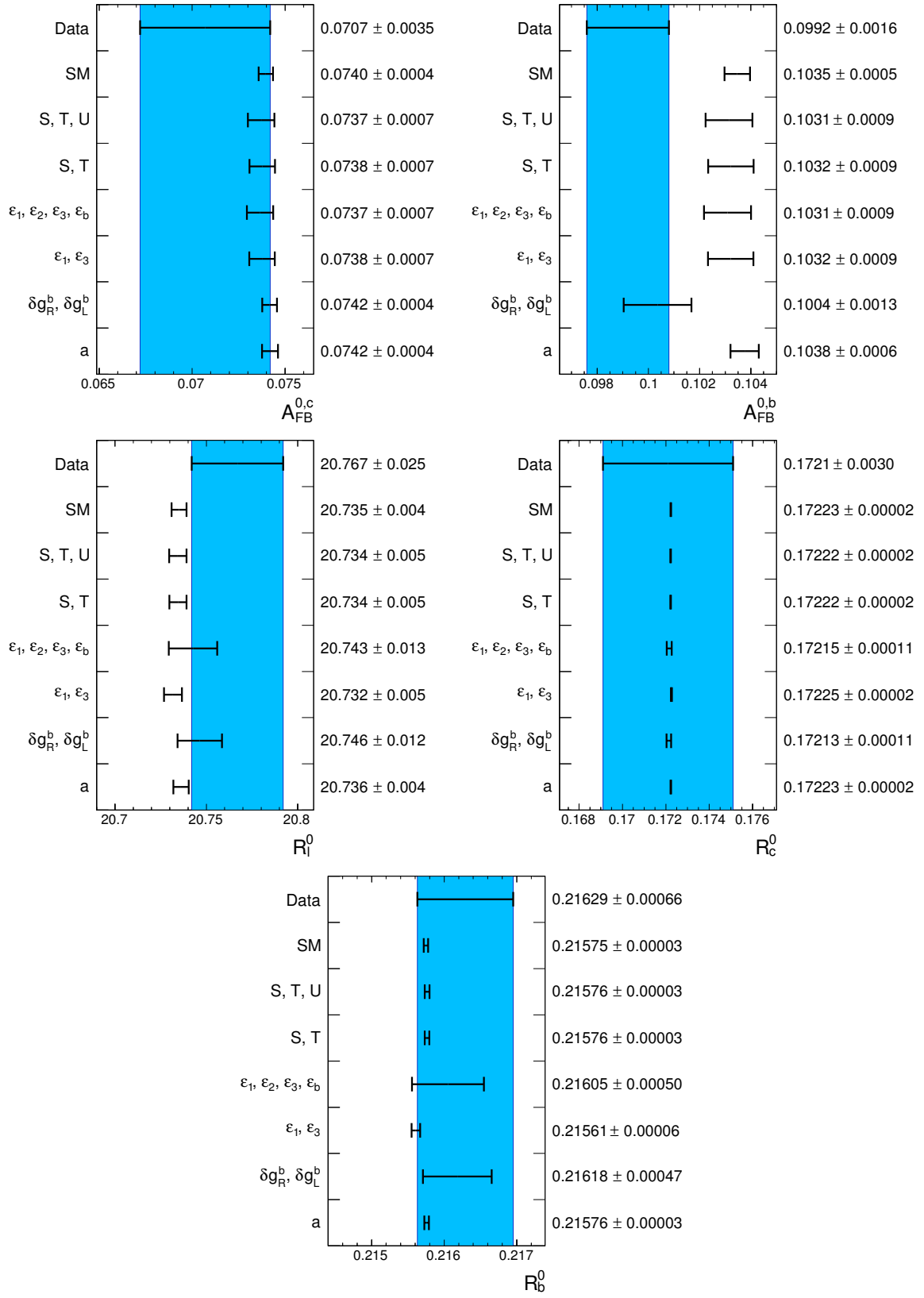


Figure 10. Same as figure 8.

E Fit results for the observables using the full two-loop fermionic EW corrections to ρ_Z^f

In this Appendix we present a graphical summary of the fit results for all observables obtained within the various scenarios considered in this work, obtained using the results from ref. [16, 83] for the two-loop fermionic EW corrections to ρ_Z^f . In the NP fits, we neglect the observables Γ_Z , σ_h^0 and R_ℓ^0 . The labels in the figures refer to the various fits performed with a self-explanatory notation. The orange band corresponds to the direct measurement, also reported with the ‘‘Data’’ label.

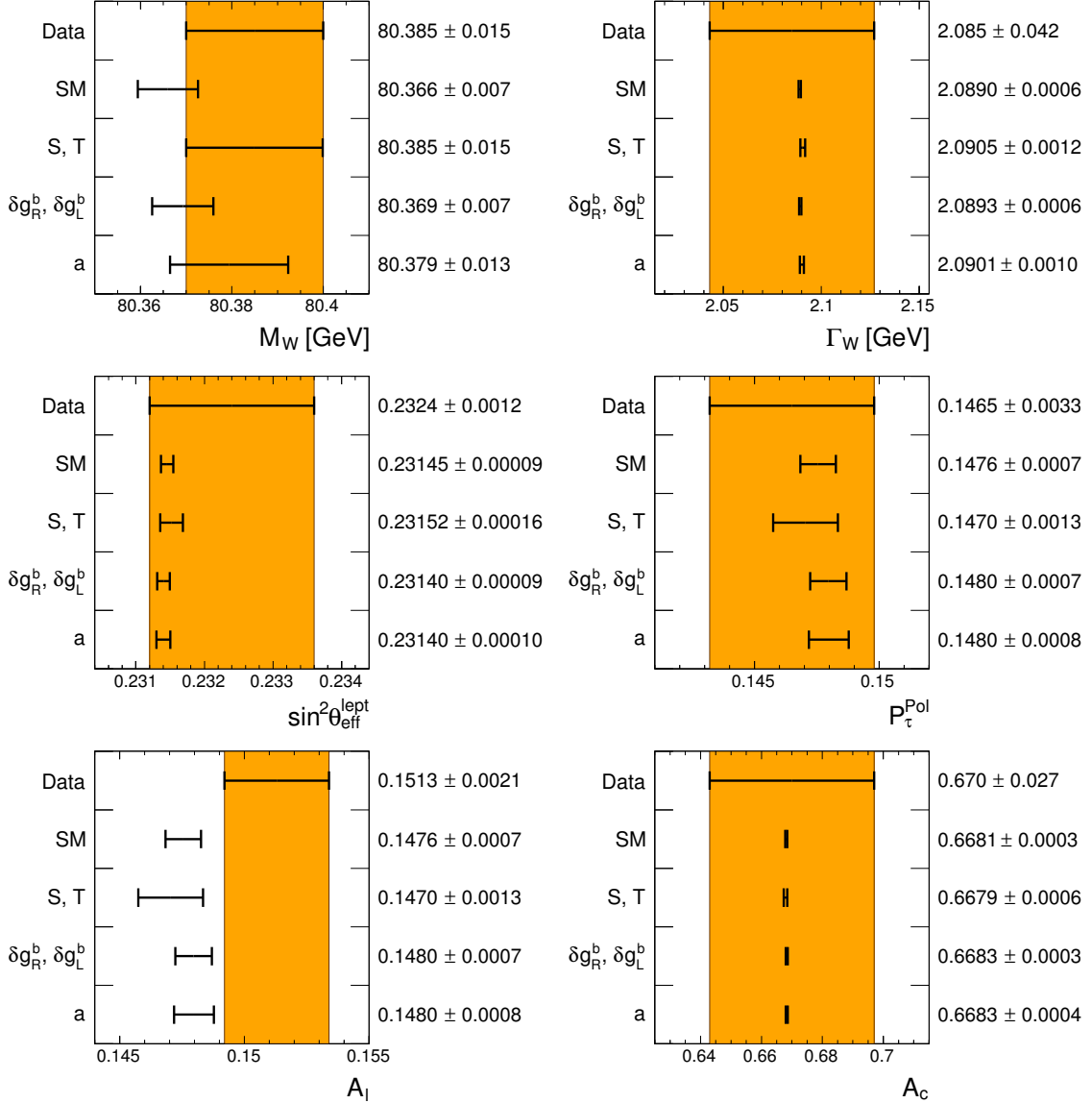


Figure 11. Fit results, including the full two-loop fermionic EW corrections to the coupling ρ_Z^f with the results of ref. [16, 83] and the parameters $\delta\rho_Z^{\nu,\ell,b}$.

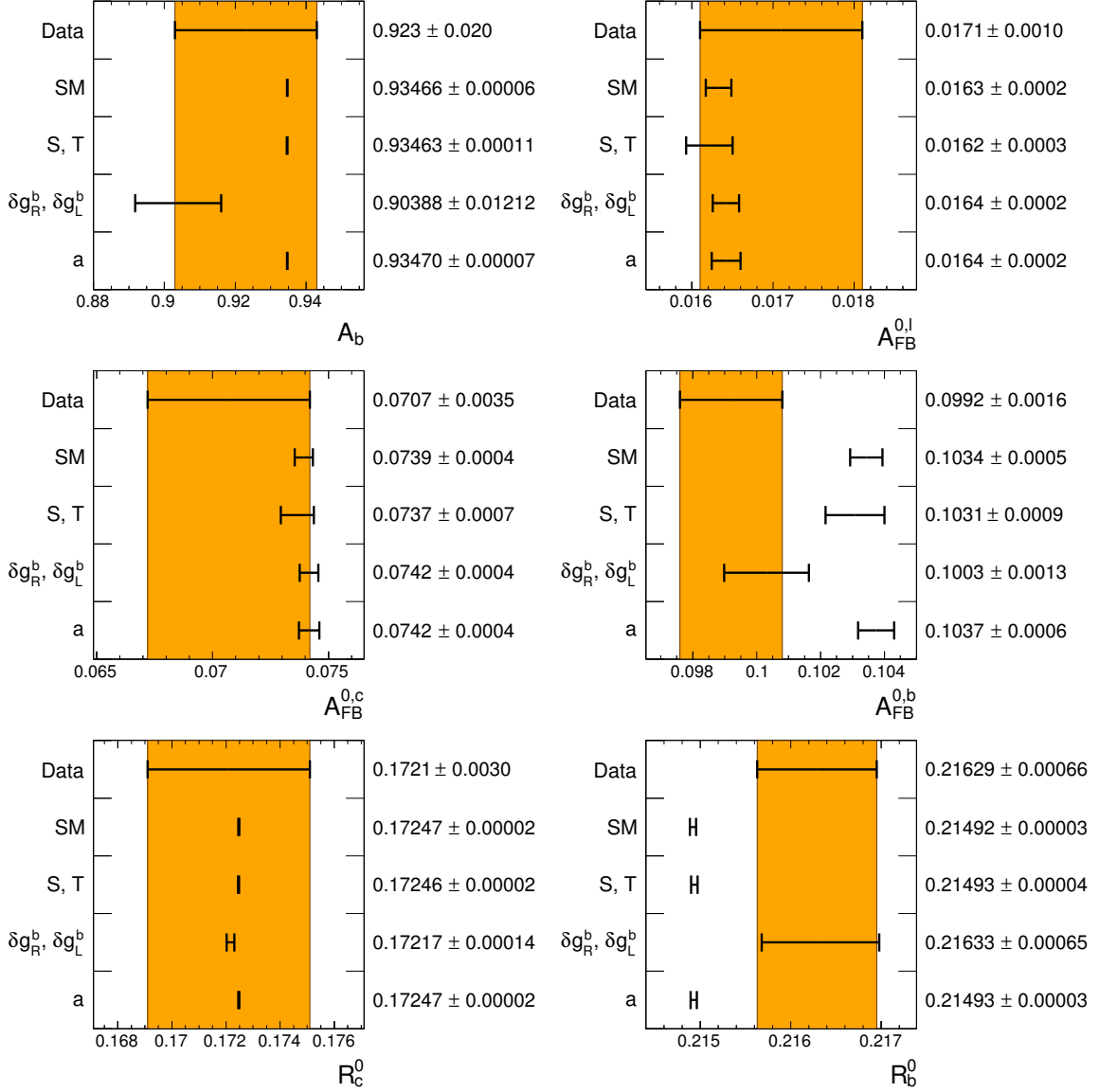


Figure 12. Same as figure 11.

References

- [1] U. Amaldi, A. Bohm, L. Durkin, P. Langacker, A. K. Mann, et al., *A comprehensive analysis of data pertaining to the weak neutral current and the intermediate vector boson masses*, *Phys.Rev.* **D36** (1987) 1385.
- [2] G. Costa, J. R. Ellis, G. L. Fogli, D. V. Nanopoulos, and F. Zwirner, *Neutral currents within and beyond the standard model*, *Nucl.Phys.* **B297** (1988) 244–286.
- [3] P. Langacker and M.-x. Luo, *Implications of precision electroweak experiments for M_t , ρ_0 , $\sin^2 \theta_W$ and grand unification*, *Phys.Rev.* **D44** (1991) 817–822.
- [4] M. E. Peskin and T. Takeuchi, *Estimation of oblique electroweak corrections*, *Phys.Rev.* **D46** (1992) 381–409.

- [5] J. Erler and P. Langacker, *Implications of high precision experiments and the CDF top quark candidates*, *Phys.Rev.* **D52** (1995) 441–450, [[hep-ph/9411203](#)].
- [6] G. Altarelli and R. Barbieri, *Vacuum polarization effects of new physics on electroweak processes*, *Phys.Lett.* **B253** (1991) 161–167.
- [7] G. Altarelli, R. Barbieri, and S. Jadach, *Toward a model independent analysis of electroweak data*, *Nucl.Phys.* **B369** (1992) 3–32; *ibid.* **B376** (1992) 444.
- [8] G. Altarelli, R. Barbieri, and F. Caravaglios, *Nonstandard analysis of electroweak precision data*, *Nucl.Phys.* **B405** (1993) 3–23.
- [9] R. Barbieri, A. Pomarol, R. Rattazzi, and A. Strumia, *Electroweak symmetry breaking after LEP1 and LEP2*, *Nucl.Phys.* **B703** (2004) 127–146, [[hep-ph/0405040](#)].
- [10] B. Grinstein and M. B. Wise, *Operator analysis for precision electroweak physics*, *Phys.Lett.* **B265** (1991) 326–334.
- [11] R. Barbieri and A. Strumia, *What is the limit on the Higgs mass?*, *Phys.Lett.* **B462** (1999) 144–149, [[hep-ph/9905281](#)].
- [12] ATLAS Collaboration, *Combined measurements of the mass and signal strength of the Higgs-like boson with the ATLAS detector using up to 25 fb⁻¹ of proton-proton collision data*, ATLAS-CONF-2013-014, ATLAS-COM-CONF-2013-025.
- [13] ATLAS Collaboration, *Observation of a new particle in the search for the Standard Model Higgs boson with the ATLAS detector at the LHC*, *Phys.Lett.* **B716** (2012) 1–29, [[arXiv:1207.7214](#)].
- [14] CMS Collaboration, *Combination of standard model Higgs boson searches and measurements of the properties of the new boson with a mass near 125 GeV*, CMS-PAS-HIG-13-005.
- [15] CMS Collaboration, *Observation of a new boson with mass near 125 GeV in pp collisions at $\sqrt{s} = 7$ and 8 TeV*, *JHEP* **06** (2013) 081, [[arXiv:1303.4571](#)].
- [16] A. Freitas and Y.-C. Huang, *Electroweak two-loop corrections to $\sin^2 \theta_{\text{eff}}^{b\bar{b}}$ and R_b using numerical Mellin-Barnes integrals*, *JHEP* **1208** (2012) 050, [[arXiv:1205.0299](#)].
- [17] G. Giudice, C. Grojean, A. Pomarol, and R. Rattazzi, *The strongly-interacting light Higgs*, *JHEP* **0706** (2007) 045, [[hep-ph/0703164](#)].
- [18] R. Contino, C. Grojean, M. Moretti, F. Piccinini, and R. Rattazzi, *Strong double Higgs production at the LHC*, *JHEP* **1005** (2010) 089, [[arXiv:1002.1011](#)].
- [19] A. Azatov, R. Contino, and J. Galloway, *Model-independent bounds on a light Higgs*, *JHEP* **1204** (2012) 127, [[arXiv:1202.3415](#)].
- [20] R. Contino, M. Ghezzi, C. Grojean, M. Muhlleitner, and M. Spira, *Effective Lagrangian for a light Higgs-like scalar*, *JHEP* **1307** (2013) 035, [[arXiv:1303.3876](#)].
- [21] A. Caldwell, D. Kollar, and K. Kroninger, *BAT: The Bayesian Analysis Toolkit*, *Comput.Phys.Commun.* **180** (2009) 2197–2209, [[arXiv:0808.2552](#)].
- [22] D. Y. Bardin, P. Christova, M. Jack, L. Kalinovskaya, A. Olchevski, et al., *ZFITTER v.6.21: A semianalytical program for fermion pair production in e^+e^- annihilation*, *Comput.Phys.Commun.* **133** (2001) 229–395, [[hep-ph/9908433](#)].
- [23] D. Y. Bardin, M. S. Bilenky, A. Chizhov, O. Fedorenko, S. N. Ganguli, et al., *ZFITTER: An analytical program for fermion pair production in e^+e^- annihilation*, [hep-ph/9412201](#).

- [24] A. Arbuzov, M. Awramik, M. Czakon, A. Freitas, M. Grunewald, et al., *ZFITTER: A semi-analytical program for fermion pair production in e^+e^- annihilation, from version 6.21 to version 6.42*, *Comput.Phys.Commun.* **174** (2006) 728–758, [[hep-ph/0507146](#)].
- [25] A. Akhundov, A. Arbuzov, S. Riemann, and T. Riemann, *ZFITTER 1985-2013*, [arXiv:1302.1395](#).
- [26] G.-C. Cho and K. Hagiwara, *Supersymmetry versus precision experiments revisited*, *Nucl.Phys.* **B574** (2000) 623–674, [[hep-ph/9912260](#)].
- [27] G.-C. Cho, K. Hagiwara, Y. Matsumoto, and D. Nomura, *The MSSM confronts the precision electroweak data and the muon $g - 2$* , *JHEP* **1111** (2011) 068, [[arXiv:1104.1769](#)].
- [28] M. Ciuchini, G. D’Agostini, E. Franco, V. Lubicz, G. Martinelli, et al., *2000 CKM triangle analysis: A critical review with updated experimental inputs and theoretical parameters*, *JHEP* **0107** (2001) 013, [[hep-ph/0012308](#)].
- [29] Particle Data Group, *Review of particle physics*, *Phys.Rev.* **D86** (2012) 010001.
- [30] S. Bethke, *World summary of α_s (2012)*, *Nucl.Phys.Proc.Suppl.* **234** (2013) 229–234, [[arXiv:1210.0325](#)].
- [31] H. Burkhardt and B. Pietrzyk, *Recent BES measurements and the hadronic contribution to the QED vacuum polarization*, *Phys.Rev.* **D84** (2011) 037502, [[arXiv:1106.2991](#)].
- [32] M. Davier, A. Hoecker, B. Malaescu, and Z. Zhang, *Reevaluation of the hadronic contributions to the muon $g - 2$ and to $\alpha(M_Z)$* , *Eur.Phys.J.* **C71** (2011) 1515, [[arXiv:1010.4180](#)].
- [33] K. Hagiwara, R. Liao, A. D. Martin, D. Nomura, and T. Teubner, *$(g - 2)_\mu$ and $\alpha(M_Z^2)$ re-evaluated using new precise data*, *J.Phys.* **G38** (2011) 085003, [[arXiv:1105.3149](#)].
- [34] F. Jegerlehner, *Electroweak effective couplings for future precision experiments*, *Nuovo Cim.* **C034S1** (2011) 31–40, [[arXiv:1107.4683](#)].
- [35] CDF and D0 Collaborations, *Combination of the top-quark mass measurements from the Tevatron collider*, *Phys.Rev.* **D86** (2012) 092003, [[arXiv:1207.1069](#)].
- [36] ATLAS and CMS Collaborations, *Combination of ATLAS and CMS results on the mass of the top quark using up to 4.9 fb^{-1} of data*, ATLAS-CONF-2012-095, CMS-PAS-TOP-12-001.
- [37] S. Alekhin, A. Djouadi, and S. Moch, *The top quark and Higgs boson masses and the stability of the electroweak vacuum*, *Phys.Lett.* **B716** (2012) 214–219, [[arXiv:1207.0980](#)].
- [38] K. Chetyrkin, B. A. Kniehl, and M. Steinhauser, *Strong coupling constant with flavor thresholds at four loops in the \overline{MS} scheme*, *Phys.Rev.Lett.* **79** (1997) 2184–2187, [[hep-ph/9706430](#)].
- [39] K. Chetyrkin, *Quark mass anomalous dimension to $O(\alpha_s^4)$* , *Phys.Lett.* **B404** (1997) 161–165, [[hep-ph/9703278](#)].
- [40] K. Chetyrkin, J. H. Kuhn, and M. Steinhauser, *RunDec: A Mathematica package for running and decoupling of the strong coupling and quark masses*, *Comput.Phys.Commun.* **133** (2000) 43–65, [[hep-ph/0004189](#)].
- [41] The LEP Electroweak Working Group. <http://lepewwg.web.cern.ch/LEPEWWG/>.
- [42] A. Sirlin, *Radiative corrections in the $SU(2)_L \times U(1)$ theory: A simple renormalization framework*, *Phys.Rev.* **D22** (1980) 971–981.

- [43] W. Marciano and A. Sirlin, *Radiative corrections to neutrino induced neutral current phenomena in the $SU(2)_L \times U(1)$ theory*, *Phys.Rev.* **D22** (1980) 2695; *ibid.* **D31** (1985) 213.
- [44] D. Y. Bardin, P. K. Khristova, and O. Fedorenko, *On the lowest order electroweak corrections to spin 1/2 fermion scattering: (I). The one-loop diagrammar*, *Nucl.Phys.* **B175** (1980) 435–461.
- [45] D. Y. Bardin, P. K. Khristova, and O. Fedorenko, *On the lowest order electroweak corrections to spin 1/2 fermion scattering: (II). The one-loop amplitudes*, *Nucl.Phys.* **B197** (1982) 1–44.
- [46] M. Awramik, M. Czakon, A. Freitas, and G. Weiglein, *Precise prediction for the W boson mass in the standard model*, *Phys.Rev.* **D69** (2004) 053006, [[hep-ph/0311148](#)].
- [47] A. Djouadi and C. Verzegnassi, *Virtual very heavy top effects in LEP/SLC precision measurements*, *Phys.Lett.* **B195** (1987) 265.
- [48] A. Djouadi, *$\mathcal{O}(\alpha\alpha_s)$ vacuum polarization functions of the standard model gauge bosons*, *Nuovo Cim.* **A100** (1988) 357.
- [49] B. A. Kniehl, *Two-loop corrections to the vacuum polarizations in perturbative QCD*, *Nucl.Phys.* **B347** (1990) 86–104.
- [50] F. Halzen and B. A. Kniehl, *Δr beyond one loop*, *Nucl.Phys.* **B353** (1991) 567–590.
- [51] B. A. Kniehl and A. Sirlin, *Dispersion relations for vacuum polarization functions in electroweak physics*, *Nucl.Phys.* **B371** (1992) 141–148.
- [52] B. A. Kniehl and A. Sirlin, *On the effect of the $t\bar{t}$ threshold on electroweak parameters*, *Phys.Rev.* **D47** (1993) 883–893.
- [53] A. Djouadi and P. Gambino, *Electroweak gauge bosons selfenergies: Complete QCD corrections*, *Phys.Rev.* **D49** (1994) 3499–3511; *ibid.* **D53** (1996) 4111, [[hep-ph/9309298](#)].
- [54] L. Avdeev, J. Fleischer, S. Mikhailov, and O. Tarasov, *$\mathcal{O}(\alpha\alpha_s^2)$ correction to the electroweak ρ parameter*, *Phys.Lett.* **B336** (1994) 560–566; *ibid.* **B349** (1995) 597–598, [[hep-ph/9406363](#)].
- [55] K. Chetyrkin, J. H. Kuhn, and M. Steinhauser, *Corrections of order $\mathcal{O}(G_F M_t^2 \alpha_s^2)$ to the ρ parameter*, *Phys.Lett.* **B351** (1995) 331–338, [[hep-ph/9502291](#)].
- [56] K. Chetyrkin, J. H. Kuhn, and M. Steinhauser, *QCD corrections from top quark to relations between electroweak parameters to order α_s^2* , *Phys.Rev.Lett.* **75** (1995) 3394–3397, [[hep-ph/9504413](#)].
- [57] R. Barbieri, M. Beccaria, P. Ciafaloni, G. Curci, and A. Vicere, *Radiative correction effects of a very heavy top*, *Phys.Lett.* **B288** (1992) 95–98, [[hep-ph/9205238](#)].
- [58] R. Barbieri, M. Beccaria, P. Ciafaloni, G. Curci, and A. Vicere, *Two-loop heavy top effects in the standard model*, *Nucl.Phys.* **B409** (1993) 105–127.
- [59] J. Fleischer, O. Tarasov, and F. Jegerlehner, *Two-loop heavy top corrections to the ρ parameter: A simple formula valid for arbitrary Higgs mass*, *Phys.Lett.* **B319** (1993) 249–256.
- [60] J. Fleischer, O. Tarasov, and F. Jegerlehner, *Two-loop large top mass corrections to electroweak parameters: Analytic results valid for arbitrary Higgs mass*, *Phys.Rev.* **D51** (1995) 3820–3837.

- [61] G. Degrandi, P. Gambino, and A. Vicini, *Two-loop heavy top effects on the m_Z - m_W interdependence*, *Phys.Lett.* **B383** (1996) 219–226, [[hep-ph/9603374](#)].
- [62] G. Degrandi, P. Gambino, and A. Sirlin, *Precise calculation of M_W , $\sin^2 \hat{\theta}_W(M_Z)$, and $\sin^2 \theta_{\text{eff}}^{\text{lept}}$* , *Phys.Lett.* **B394** (1997) 188–194, [[hep-ph/9611363](#)].
- [63] G. Degrandi and P. Gambino, *Two-loop heavy top corrections to the Z^0 boson partial widths*, *Nucl.Phys.* **B567** (2000) 3–31, [[hep-ph/9905472](#)].
- [64] A. Freitas, W. Hollik, W. Walter, and G. Weiglein, *Complete fermionic two-loop results for the M_W - M_Z interdependence*, *Phys.Lett.* **B495** (2000) 338–346; *ibid.* **B570** (2003) 260–264, [[hep-ph/0007091](#)].
- [65] A. Freitas, W. Hollik, W. Walter, and G. Weiglein, *Electroweak two-loop corrections to the M_W - M_Z mass correlation in the standard model*, *Nucl.Phys.* **B632** (2002) 189–218; *ibid.* **B666** (2003) 305–307, [[hep-ph/0202131](#)].
- [66] M. Awramik and M. Czakon, *Complete two loop bosonic contributions to the muon lifetime in the standard model*, *Phys.Rev.Lett.* **89** (2002) 241801, [[hep-ph/0208113](#)].
- [67] A. Onishchenko and O. Veretin, *Two-loop bosonic electroweak corrections to the muon lifetime and M_Z - M_W interdependence*, *Phys.Lett.* **B551** (2003) 111–114, [[hep-ph/0209010](#)].
- [68] M. Awramik, M. Czakon, A. Onishchenko, and O. Veretin, *Bosonic corrections to Δr at the two loop level*, *Phys.Rev.* **D68** (2003) 053004, [[hep-ph/0209084](#)].
- [69] M. Awramik and M. Czakon, *Two loop electroweak bosonic corrections to the muon decay lifetime*, *Nucl.Phys.Proc.Suppl.* **116** (2003) 238–242, [[hep-ph/0211041](#)].
- [70] M. Awramik and M. Czakon, *Complete two loop electroweak contributions to the muon lifetime in the standard model*, *Phys.Lett.* **B568** (2003) 48–54, [[hep-ph/0305248](#)].
- [71] J. van der Bij, K. Chetyrkin, M. Faisst, G. Jikia, and T. Seidensticker, *Three-loop leading top mass contributions to the ρ parameter*, *Phys.Lett.* **B498** (2001) 156–162, [[hep-ph/0011373](#)].
- [72] M. Faisst, J. H. Kuhn, T. Seidensticker, and O. Veretin, *Three loop top quark contributions to the ρ parameter*, *Nucl.Phys.* **B665** (2003) 649–662, [[hep-ph/0302275](#)].
- [73] G. Weiglein, *Results for precision observables in the electroweak standard model at two-loop order and beyond*, *Acta Phys.Polon.* **B29** (1998) 2735–2741, [[hep-ph/9807222](#)].
- [74] R. Boughezal, J. Tausk, and J. van der Bij, *Three-loop electroweak correction to the ρ parameter in the large Higgs mass limit*, *Nucl.Phys.* **B713** (2005) 278–290, [[hep-ph/0410216](#)].
- [75] R. Boughezal, J. Tausk, and J. van der Bij, *Three-loop electroweak corrections to the W -boson mass and $\sin^2 \theta_{\text{eff}}^{\text{lept}}$ in the large Higgs limit*, *Nucl.Phys.* **B725** (2005) 3–14, [[hep-ph/0504092](#)].
- [76] Y. Schroder and M. Steinhauser, *Four-loop singlet contribution to the ρ parameter*, *Phys.Lett.* **B622** (2005) 124–130, [[hep-ph/0504055](#)].
- [77] K. Chetyrkin, M. Faisst, J. H. Kuhn, P. Maierhofer, and C. Sturm, *Four-loop QCD corrections to the ρ parameter*, *Phys.Rev.Lett.* **97** (2006) 102003, [[hep-ph/0605201](#)].
- [78] R. Boughezal and M. Czakon, *Single scale tadpoles and $O(G_F m_t^2 \alpha_s^3)$ corrections to the ρ parameter*, *Nucl.Phys.* **B755** (2006) 221–238, [[hep-ph/0606232](#)].

- [79] D. Y. Bardin and G. Passarino, *The standard model in the making: Precision study of the electroweak interactions*, Oxford University Press (1999) 685 p.
- [80] M. Awramik, M. Czakon, A. Freitas, and G. Weiglein, *Complete two-loop electroweak fermionic corrections to $\sin^2 \theta_{\text{eff}}^{\text{lep,t}}$ and indirect determination of the Higgs boson mass*, *Phys.Rev.Lett.* **93** (2004) 201805, [[hep-ph/0407317](#)].
- [81] M. Awramik, M. Czakon, and A. Freitas, *Electroweak two-loop corrections to the effective weak mixing angle*, *JHEP* **0611** (2006) 048, [[hep-ph/0608099](#)].
- [82] M. Awramik, M. Czakon, A. Freitas, and B. Kniehl, *Two-loop electroweak fermionic corrections to $\sin^2 \theta_{\text{eff}}^{bb}$* , *Nucl.Phys.* **B813** (2009) 174–187, [[arXiv:0811.1364](#)].
- [83] A. Freitas. Private communication.
- [84] ALEPH, DELPHI, L3, OPAL, SLD Collaborations, LEP Electroweak Working Group, and SLD Electroweak and Heavy Flavour Groups, *Precision electroweak measurements on the Z resonance*, *Phys.Rept.* **427** (2006) 257–454, [[hep-ex/0509008](#)].
- [85] ALEPH, CDF, D0, DELPHI, L3, OPAL, SLD Collaborations, LEP Electroweak Working Group, Tevatron Electroweak Working Group, and SLD Electroweak and Heavy Flavour Groups, *Precision electroweak measurements and constraints on the standard model*, [[arXiv:1012.2367](#)].
- [86] K. Chetyrkin, J. H. Kuhn, and A. Kwiatkowski, *QCD corrections to the e^+e^- cross-section and the Z boson decay rate*, [[hep-ph/9503396](#)].
- [87] P. Baikov, K. Chetyrkin, J. Kuhn, and J. Rittinger, *Complete $\mathcal{O}(\alpha_s^4)$ QCD corrections to hadronic Z-decays*, *Phys.Rev.Lett.* **108** (2012) 222003, [[arXiv:1201.5804](#)].
- [88] A. Czarnecki and J. H. Kuhn, *Nonfactorizable QCD and electroweak corrections to the hadronic Z boson decay rate*, *Phys.Rev.Lett.* **77** (1996) 3955–3958, [[hep-ph/9608366](#)].
- [89] R. Harlander, T. Seidensticker, and M. Steinhauser, *Complete corrections of $\mathcal{O}(\alpha\alpha_s)$ to the decay of the Z boson into bottom quarks*, *Phys.Lett.* **B426** (1998) 125–132, [[hep-ph/9712228](#)].
- [90] D. Y. Bardin, S. Riemann, and T. Riemann, *Electroweak one-loop corrections to the decay of the charged vector boson*, *Z.Phys.* **C32** (1986) 121–125.
- [91] The Tevatron Electroweak Working Group for the CDF and D0 Collaborations, *2012 update of the combination of CDF and D0 results for the mass of the W boson*, [[arXiv:1204.0042](#)].
- [92] UTfit Collaboration, *The 2004 UTfit collaboration report on the status of the unitarity triangle in the standard model*, *JHEP* **0507** (2005) 028, [[hep-ph/0501199](#)].
- [93] J. Erler, *Tests of the electroweak standard model*, [[arXiv:1209.3324](#)].
- [94] O. Eberhardt et al., *Impact of a Higgs boson at a mass of 126 GeV on the standard model with three and four fermion generations*, *Phys.Rev.Lett.* **109** (2012) 241802, [[arXiv:1209.1101](#)].
- [95] M. Baak, M. Goebel, J. Haller, A. Hoecker, D. Kennedy, et al., *The electroweak fit of the standard model after the discovery of a new boson at the LHC*, *Eur.Phys.J.* **C72** (2012) 2205, [[arXiv:1209.2716](#)].
- [96] M. Baak and R. Kogler, *The global electroweak Standard Model fit after the Higgs discovery*, [[arXiv:1306.0571](#)].

- [97] D. Kennedy and B. Lynn, *Electroweak radiative corrections with an effective Lagrangian: Four fermion processes*, *Nucl.Phys.* **B322** (1989) 1–54.
- [98] D. Kennedy, B. Lynn, C. Im, and R. Stuart, *Electroweak cross-sections and asymmetries at the Z^0* , *Nucl.Phys.* **B321** (1989) 83.
- [99] M. E. Peskin and T. Takeuchi, *A new constraint on a strongly interacting Higgs sector*, *Phys.Rev.Lett.* **65** (1990) 964–967.
- [100] I. Maksymyk, C. Burgess, and D. London, *Beyond S , T and U* , *Phys.Rev.* **D50** (1994) 529–535, [[hep-ph/9306267](#)].
- [101] C. Burgess, S. Godfrey, H. Konig, D. London, and I. Maksymyk, *A global fit to extended oblique parameters*, *Phys.Lett.* **B326** (1994) 276–281, [[hep-ph/9307337](#)].
- [102] C. Burgess, S. Godfrey, H. Konig, D. London, and I. Maksymyk, *Model independent global constraints on new physics*, *Phys.Rev.* **D49** (1994) 6115–6147, [[hep-ph/9312291](#)].
- [103] G. Altarelli, R. Barbieri, and F. Caravaglios, *The epsilon variables for electroweak precision tests: A reappraisal*, *Phys.Lett.* **B349** (1995) 145–154.
- [104] G. Altarelli, R. Barbieri, and F. Caravaglios, *Electroweak precision tests: A concise review*, *Int.J.Mod.Phys.* **A13** (1998) 1031–1058, [[hep-ph/9712368](#)].
- [105] P. Bamert, C. Burgess, J. M. Cline, D. London, and E. Nardi, *R_b and new physics: A comprehensive analysis*, *Phys.Rev.* **D54** (1996) 4275–4300, [[hep-ph/9602438](#)].
- [106] H. E. Haber and H. E. Logan, *Radiative corrections to the $Zb\bar{b}$ vertex and constraints on extended Higgs sectors*, *Phys.Rev.* **D62** (2000) 015011, [[hep-ph/9909335](#)].
- [107] D. Choudhury, T. M. Tait, and C. Wagner, *Beautiful mirrors and precision electroweak data*, *Phys.Rev.* **D65** (2002) 053002, [[hep-ph/0109097](#)].
- [108] K. Agashe, R. Contino, L. Da Rold, and A. Pomarol, *A custodial symmetry for $Zb\bar{b}$* , *Phys.Lett.* **B641** (2006) 62–66, [[hep-ph/0605341](#)].
- [109] A. Djouadi, G. Moreau, and F. Richard, *Resolving the A_{FB}^b puzzle in an extra dimensional model with an extended gauge structure*, *Nucl.Phys.* **B773** (2007) 43–64, [[hep-ph/0610173](#)].
- [110] K. Kumar, W. Shepherd, T. M. Tait, and R. Vega-Morales, *Beautiful mirrors at the LHC*, *JHEP* **1008** (2010) 052, [[arXiv:1004.4895](#)].
- [111] F. del Aguila, J. de Blas, and M. Perez-Victoria, *Electroweak limits on general new vector bosons*, *JHEP* **1009** (2010) 033, [[arXiv:1005.3998](#)].
- [112] L. Da Rold, *Solving the A_{FB}^b anomaly in natural composite models*, *JHEP* **1102** (2011) 034, [[arXiv:1009.2392](#)].
- [113] E. Alvarez, L. Da Rold, and A. Szykman, *A composite Higgs model analysis of forward-backward asymmetries in the production of tops at Tevatron and bottoms at LEP and SLC*, *JHEP* **1105** (2011) 070, [[arXiv:1011.6557](#)].
- [114] R. Dermisek, S.-G. Kim, and A. Raval, *New vector boson near the Z-pole and the puzzle in precision electroweak data*, *Phys.Rev.* **D84** (2011) 035006, [[arXiv:1105.0773](#)].
- [115] A. Djouadi, G. Moreau, and F. Richard, *Forward-backward asymmetries of the bottom and top quarks in warped extra-dimensional models: LHC predictions from the LEP and Tevatron anomalies*, *Phys.Lett.* **B701** (2011) 458–464, [[arXiv:1105.3158](#)].

- [116] R. Dermisek, S.-G. Kim, and A. Raval, *Z' near the Z-pole*, *Phys.Rev.* **D85** (2012) 075022, [[arXiv:1201.0315](#)].
- [117] B. Batell, S. Gori, and L.-T. Wang, *Higgs couplings and precision electroweak data*, *JHEP* **1301** (2013) 139, [[arXiv:1209.6382](#)].
- [118] D. Guadagnoli and G. Isidori, *B($B_s \rightarrow \mu^+ \mu^-$) as an electroweak precision test*, [arXiv:1302.3909](#).
- [119] R. Barbieri, B. Bellazzini, V. S. Rychkov, and A. Varagnolo, *The Higgs boson from an extended symmetry*, *Phys.Rev.* **D76** (2007) 115008, [[arXiv:0706.0432](#)].
- [120] A. Falkowski, S. Rychkov, and A. Urbano, *What if the Higgs couplings to W and Z bosons are larger than in the Standard Model?*, *JHEP* **1204** (2012) 073, [[arXiv:1202.1532](#)].
- [121] A. Falkowski, F. Riva, and A. Urbano, *Higgs at last*, [arXiv:1303.1812](#).
- [122] C. Grojean, O. Matsedonskyi, and G. Panico, *Light top partners and precision physics*, [arXiv:1306.4655](#).
- [123] W. Buchmuller and D. Wyler, *Effective Lagrangian analysis of new interactions and flavor conservation*, *Nucl.Phys.* **B268** (1986) 621.
- [124] F. del Aguila and J. de Blas, *Electroweak constraints on new physics*, *Fortsch.Phys.* **59** (2011) 1036–1040, [[arXiv:1105.6103](#)].
- [125] C. Grojean, E. E. Jenkins, A. V. Manohar, and M. Trott, *Renormalization group scaling of Higgs operators and $\Gamma(h \rightarrow \gamma\gamma)$* , *JHEP* **1304** (2013) 016, [[arXiv:1301.2588](#)].
- [126] J. Elias-Miró, J. Espinosa, E. Masso, and A. Pomarol, *Renormalization of dimension-six operators relevant for the Higgs decays $h \rightarrow \gamma\gamma, \gamma Z$* , *JHEP* **1308** (2013) 033, [[arXiv:1302.5661](#)].
- [127] E. E. Jenkins, A. V. Manohar, and M. Trott, *On gauge invariance and minimal coupling*, [arXiv:1305.0017](#).